Response to Referee number 3

The authors thank Referee #3 for his/her expertise and valuable comments to further improve and clarify the MS. We have considered all recommendations and made appropriate alterations. Our specific responses to the comments are as follows, while the detailed textual modifications were amended in the marked-up version of the MS ver. 3.

The authors claim" daily activity time pattern of inhabitants determine many atmospheric sources and important processes". However, they choose UTC+1 throughout the year to characterize the starting time of NPF. In addition, Figure 4 clearly shows that radiation has an important impact on the particle formation and growth process. All this is contradictory to their statement. With their approach they find that "nucleation ordinarily starts at 09:15 UTC+1". I doubt that this result is very helpful for e.g. modelers, if they know that nucleation can happen sometime between 6 – 12 a.m. Of interest would be some information on the underlying process/drivers.

1. It is the direct emissions mainly from vehicular road traffic, some household activities and service sectors that follow the daily activity time pattern of inhabitants (Paasonen et al., ACP, 16, 6823–6840, 2016). These sources determine many atmospheric processes in cities in general. Local time (LT) scale is often used for them. We must stress the role of meteorology as well. Urban atmospheric NPF and growth events take place in this dynamic atmospheric environment, and they are associated with several precursors of both anthropogenic and biogenic origin, further secondary chemical species and meteorological conditions. Since the impact of GRad seems to be important and biogenic emissions may also strongly influence the whole process, and since both these effects are influenced by solar cycling, we expressed the starting time parameter t_1 of NPF in UTC+1. This also facilitates its descriptive statistics and its comparison among different environments. (In LT, this would be misleading.) We do not see contradiction here. It is not completely clear where the interval of 06:00–12:00 came from; the NPF events in Budapest (as representative of a large Central European city) start between 08:00 and 10:50 UTC+1 in the centre, and between about 07:10 and 09:30 UTC+1 in the near-city background with average values given in Table 2, and there is a delay of about 1 h in urban NPF with respect to its close background. This could interest modellers.

Line 266-270: this is an incomplete sentence. Probably you need to delete "and which"

2. The sentence mentioned was split into 2 parts to clarify its exact meaning and to help more fluent reading.

Line 274-275: These explain….. This sentence is not clear.

3. The sentence was improved by an explicit grammatical subject.

Line 318-319: the factor could distort the dynamic relationships …. It could also be that neglecting this factor leads to a bias. It can be either way.

4. The part of the sentence was removed. These factors are basically related to the limitations of the proxy value.

Line 506-508: this sentence is unclear. Why should there be a seasonal bias? I assume you compare event and non-event days per month. Otherwise it does not make sense.
Line 508: I do not see a seasonal cycle for CS.

5. The sentences mentioned were extended with further aspects to clarify their meaning.

Line 526: "uncertainty", should this not be variability?

6. We referred to the standard deviations of the monthly mean values, which are expected to become smaller as the length of the data set gets larger.

Line 542: "higher biogenic emissions and typically stronger photochemistry are expected" higher photochemical activity also enhances formation of nucleating species from anthropogenic VOCs. It must not necessarily be biogenic species.

7. The sentence was reformulated to clarify that we originally meant 2 processes of 1) higher biogenic emissions and 2) stronger photochemistry as separate contributors. The latter process enhances the production of nucleating chemical species from both biogenic and non-biogenic (e.g., anthropogenic) sources.

Line 544: "nothing extra that would suppress the dynamical properties". This is not fully correct. Higher T in summer leads to higher vapor pressure and decreases supersaturation. This decreases nucleation and growth rates.

8. The sentence (more precisely "practically nothing extra…") was cited from Kerminen et al., 2018, and the effect of T mentioned was taken into account as an ordinary impact. We modified the formulation to clarify undergoing processes in more detail.

Line 666: In line 467 you estimate H2SO4 to 5E05 cm-3. 12.3% of growth by H2SO4 results in about 1 nm/h. This would need about 5E07 H2SO4. How do you explain this discrepancy of 2 orders of magnitude?

9. It is not fully straightforward to follow the requirement of the H_2SO_4 concentration of 5×10^7 cm^{-3} from the comment. The difference could be caused by the scaling factor as discussed in lines 316–320 of the MS ver. 2. Atmospheric measurements of H_2SO_4 by an CI APi-TOF MS on the spot in last spring also indicate values around 7×10^5 cm^{-3}.

Line 668: what do you mean with "excess"? "formation of H2SO4 is likely governed by photochemical conditions": what other processes than photochemical production could do it under the given urban conditions?

10. We utilized the expression "in excess" in its chemical sense, thus, meaning that it is usually not the lack of SO_2 gas itself, which limits the NPF and growth events in Budapest, and that the conditions for photochemical oxidation of SO_2 to H_2SO_4 (its reaction rate in the gas phase) could be one of the governing process. The related sentences were modified.

Line 794: replace cloud by CLOUD. You need to say what this is.

11. We referred to cloud chamber experiments in general including likely the most outstanding facility of CLOUD at CERN. The sentence was removed for another reason.

The writing of the text is still quite complicated and not so concise. English needs substantial improvement yet.

12. Several sentences were split into shorter parts. The writing and language of the MS was improved.

Imre Salma

Response to Referee number 5

The authors thank Referee #5 for his/her work. The Referee's report is very short, and it contains only 1 real issue. This is, unfortunately, based on a misunderstanding of the objectives of the MS. Our responses are as follows, while the detailed textual modifications were amended in the marked-up version of the MS ver. 3.

The dataset presented consist of several years of urban aerosol dynamics data. However, the data analysis presented is too simple – only average values, standard deviations and linear regressions are discussed, and the uncertainties are too large to draw robust conclusions in many cases. Overall, the authors should consider a different approach to the data analysis in order to draw interesting and substantial conclusions from the dataset.

1. In the present MS, we mainly focused on various aspects of dynamic and timing properties. The objectives include for instance: 1) the evaluation and discussion of monthly distributions of J_6 an GR_{10} together with their relationships with nucleation occurrence frequency and relevant atmospheric parameters, 2) timing properties of NPF and growth events, 3) refinements of J and GR calculations dedicated to urban environments, 4) statistical distributions of J_6 an GR_{10}, 5) occurrence and properties of extreme events and events with broad onset. These items represent considerable novelty and new knowledge.

   The objectives do not include the data analysis raised by the Referee. The overall extent of the data base available by now is estimated to contain critically evaluated records/lines for 7 measurement years, which each consists of size distribution data in 27 channels with a time resolution of ca. 8 min, particle number concentrations for 4 different size fractions ($N_{6–25}$, $N_{6–100}$=UF, $N_{100–1000}$ and N), 2 derived compound properties (CS and H_2SO_4 proxy), 5 meteorological data (T, RH, WS, WD and GRad with a time resolution of 10 min), concentrations of 5 pollutant gases (SO_2, NO, NO_x, O_3 and CO with a time resolution of 1 h) and attribution indices on the nucleation classes and workdays/holidays. Its comprehensive analysis requires specific and careful adaptation of multivariate statistical methods. We have been working on this in a separate project in cooperation with dedicated mathematical statisticians, and its results and conclusions are to be published in a new MS later.

Additionally, it does not make sense to mix a 5-year-long dataset for the city center with a 1-year-long dataset for the near-city site into the same data analysis.

2. The NPF and growth processes in the city centre and near-city background environments were almost exclusively evaluated separately (see Tables 1 and 2, Figs. 2 and 3 for summary). We showed previously (Salma et al., ACP, 2016b) that the NPF events observed in the city centre of Budapest and its background usually happen above a larger territory in the Carpathian Basin as a spatially coherent and joint atmospheric phenomenon. From this aspect only and in selected specific cases such as the relative occurrence frequency distribution, the data sets for the centre and near-city background were joined and treated together in the first approximation. This was explicitly stated and argued for (lines 359–363 of the MS ver. 2). Nevertheless, we evaluated the average frequency distributions separately as well and found no substantial or tendentious differences in the distributions averaged for the overall data set, city centre data set and near-city background data set. This information was added to the MS ver. 3.

Furthermore, the title does not match the contents of the manuscript.

3. The title was changed to express the content of the MS more closely.

In summary, we were able to find a positive message in this comment. We can fully agree with the Referee on the importance and necessity of further complex statistical analysis, and we regard the comment as an initiation or confirmation that we should continue in this way. At the same time, the major research results of the present MS (such as the items 1–5 listed above) should not be neglected and are to be considered as well when making the final decision.

Imre Salma

Response to Referee number 6

The authors thank Referee #6 for his/her detailed, expertise and valuable comments to further improve and clarify the MS. We have considered all recommendations and made appropriate alterations. Our specific responses to the comments are as follows, while the detailed textual modifications were amended in the marked-up version of the MS ver. 3.

The title must be changed reflecting the real scope of the study.

1. The title was changed to express the content of the MS more closely.

Conclusions should be stated taking into account the limitations of the method employed. Some of sentences stated in the abstract ("The 15 NPF and growth events produce 4.6 aerosol particles with a diameter of 6 nm in 1 cm3 of air in 16 1 s…") and in the conclusion sections must be modified taking into account the limitations of the methodology and the scope of the study. The conclusion section does not exactly reflect the results obtained during this study. Thus, the present study did not provide information about effect of NPF in urban climate and health risk (l774-776). Cited form text (L792-793): "the present research…provided evidence that some important chemical players in the NPF and growth events are still missing". This cannot be considered as a conclusion obtained in this paper. The methodology used does not permit to identify key chemical players because the methods used are not the most adequate to this end.

2. The sentences cited from the Conclusions were meant as an outlook for further directions. To avoid any misunderstanding, we removed or modified substantially them. In addition, several other statements were reformulated into more modest expressions to insist more on the direct implications. In addition, the methodological limitations of the study were emphasized in the body of the MS ver. 3.

The statically treatment can be improved. The analysis should be performed for both the NPF and non-NPF events. Thus, in Section 4-2 and Figure 2, the analysis of the monthly evolution is limited to the NPF formation events. It should also be performed for the non-NPF events. A figure about daily evolution of NPF events, and other variables, could help for interpretation.

3. Following the comment of the Referee, we performed completely new calculations for the non-NPF event days, derived average NPF event day-to-non-event day ratios for all variables, discussed and interpreted them in a completely new paragraph in Sect. 4.2, and

added a new Fig. 3 on monthly distribution of the most important variables in 10 panels. Thank to the Referee's comment, these results revealed new aspects of the penomenon. Full exploitation of the overall data set by multistatistical and other methods - including among others the diurnal variations - has been going on in a separate project.

English grammar is good, but sentences are quite long and, frequently do no provide useful information. The length of the text must be shorted (27 pages, without references with only 3 figures and 3 tables).

4. Several sentences were split into parts; the writing and language of the MS was improved, and the MS was shortened. Figures 2 and 4 consist of 4 and 6 panels, respectively, while the supplementary material contains 3 more tables and 2 more figures. We also prepared a new Fig. 3 consisting of 10 panels.

Section 4-2 and Figure 2: It is surprising the monthly evolution of NOx and SO2. Information about DL for SO2 should be provided. Monthly and daily evolution for both NPF and non-NPF events would also provide info about it.

5. The concentration of SO_2 in the Budapest area is ordinarily distributed without larger spatial gradients. It suggests that it is usually available for the NPF process. Its monthly average concentrations for NPF and non-NPF days were identical within the uncertainty intervals. The limit of determination (LOD) of the SO_2 analyser system applied is approximately $0.2\ \mu g\ m^{-3}$. More than 98% of the hourly-mean concentrations were above the LOD. The requested information was added to the text. See also response no. 12.

Section 4.4. As it is do not provide very useful information.

6. Several sentences in this section were removed or shortened.

Methodology: sampling performed at two sites with different inlet configuration; were the particle loses corrected?

7. It was the same experimental system that was deployed at both measurement sites. The inlet tubing (its material, internal and outer diameters, curvature, rain cover, insect net and length) was identical and the DMPS was also the same. It is, therefore, expected that the particle losses in the 2 configurations were very similar. A short note on this was added.

Table 1: add annual mean concentrations in Table 1, and simplify the description in the beginning of section 4.

8. The concentrations were replaced from the text to Table 1 as requested and the corresponding part of the text could indeed be largely shortened and simplified.

Line 341: define range for UF and N (UF/N)

9. All size fractions of aerosol particles were defined in lines 171–172 of the MS ver. 2.

Figure captions: can be simplified; too long

10. We simplified or shortened the captions. They should, however, remain self-explanatory, particularly for figures consisting of several panels.

Page 14; lines 439-441: This statement is not directly deduced from the observations.

11. The statement was removed.

Figure 2: scale for NOx and SO2

12. Gas SO_2 is a major precursor for NPF and growth events, while there are indications that NO_x can play a suppressing roles in the process. Their concentrations as shown in Fig. 2d for NPF days exhibited largely constant time behaviour. It was indicated by the variability of their monthly medians around the annual median (constant line). Despite this dependency, we would like to keep displaying them as well because atmospheric "observations in this regard are inconclusive" and "there are contrasting observations" (Kerminen et al., 2018). We showed here and are to emphasize by Fig. 2d that in the Budapest area, these gases have limited influence on atmospheric NPF events. The related text was also extended by this information.

Page 26. Lines 774-776: it cannot be inferred from the cited example that NPF can affect urban climate and health risk

13. These lines contain an outlook. They were modified to further emphasize this character.

Page26; rows 792-793: the present research does not permit to identify key chemical players because the methods used e not the most adequate to do it.

14. The sentence was removed.

Imre Salma

1 ~~Consequences of d~~Dynamic and timing properties of
2 new aerosol particle formation and consecutive growth events

3 Imre Salma and Zoltán Németh

4 Institute of Chemistry, Eötvös University, H-1518 Budapest, P.O. Box 32, Hungary

5 Correspondence to: Imre Salma (salma@chem.elte.hu)

6 **Abstract.** ~~A variety of contributions to the emerging research field of urban atmospheric new~~
7 ~~particle formation (NPF) and consecutive particle diameter growth based on gradually~~
8 ~~generating, several-year long, semi-continuous, critically evaluated, complex and coherent data~~
9 ~~sets are presented here.~~ Dynamic properties, i.e. particle formation rate J_6 and particle diameter
10 growth rate GR_{10}, and timing properties, i.e. starting time (t_1) and duration time interval (Δt) of
11 247 quantifiable atmospheric NPF and growth events identified in the city centre and near-city
12 background of Budapest over 6 full measurement years together with related gas-phase H_2SO_4
13 proxy, condensation sink (CS) of vapours, basic meteorological data and concentrations of
14 criteria pollutant gases were derived, evaluated, discussed and interpreted. In the city centre,
15 nucleation ordinarily starts at 09:15 UTC+1, and it is maintained for approximately 3 h. The
16 NPF and growth events produce 4.6 aerosol particles with a diameter of 6 nm in 1 cm^3 of air in
17 1 s, and cause the particles with a diameter of 10 nm to grow with a typical rate of 7.3 nm h^{-1}.
18 Nucleation starts approximately 1 h earlier in the near-city background, it shows substantially
19 smaller J_6 (with a median of 2.0 cm^{-3} s^{-1}) and GR_{10} values (with a median of 5.0 nm h^{-1}), while
20 the duration of nucleation is similar to that in the centre. Monthly distributions of the dynamic
21 properties and daily maximum H_2SO_4 proxy do not follow the mean monthly pattern of the
22 event occurrence frequency. The factors that control the event occurrence and that govern the
23 intensity of particle formation and growth are not directly linked. New particle formation and
24 growth processes advance in a different manner in the city and its close environment. This could
25 likely be related to diversities in atmospheric composition, chemistry and physics. ~~We showed~~
26 ~~that there is a minimum growth rate (1.8 nm h^{-1} is our case) that is required for nucleated~~
27 ~~particles to reach the lower end of the diameter interval measured (in our case 6 nm).~~ Monthly
28 distributions and relationships among the properties mentioned provided indirect evidence that
29 chemical species other than H_2SO_4 largely influence the particle growth and possibly
30 atmospheric NPF process as well. The J_6, GR_{10} and Δt can be described by log-normal
31 distribution function. Most of the extreme dynamic properties could not be explained by ~~H_2SO_4~~

32 ~~proxy, CS, meteorological data or pollutant gas concentrations~~available single or compound

33 variables. Approximately 40% of the NPF and growth events exhibited broad beginning, which

34 can be an urban feature. For ~~ca. 10% of all quantifiable event days, it was feasible to calculate~~

35 ~~2 separate sets of dynamic properties. T~~doublets, the later onset frequently shows more

36 intensive particle formation and growth than the first onset by a typical factor of approximately

37 1.5. The first event is attributed to regional type, while the second event, superimposed on the

38 first, is often associated with sub-regional, thus urban NPF and growth process.

39

40 **1 Introduction**

41

42 Molecules and molecular fragments in the air collide randomly and can form electrically neutral

43 or charged clusters. Most clusters decompose shortly. Chemical stabilising interactions among

44 certain components within a cluster can enhance its lifetime, during which it can grow further

45 by additional molecular collisions through some distinguishable size regimes (Kulmala et al.,

46 2014). If the diameter of these clusters reaches a critical value of 1.5±0.3 nm (Kulmala et al.,

47 2013), they become thermodynamically stable, and their further growth turns into a spontaneous

48 process. Supersaturation is a necessary atmospheric condition for this principal transformation.

49 It is essentially a phase transition, which takes place in a dispersed manner in the atmosphere,

50 so it generates an aerosol system. The newly formed particles grow further by condensation to

51 larger sizes in most cases due to the existing supersaturation. Photochemical oxidation products

52 such as H_2SO_4 (Sipilä et al., 2010), extremely low-volatile organic compounds (ELVOCs, Ehn

53 et al., 2014; Jokinen et al., 2015) and highly oxygenated molecules (HOMs, Bianchi et al., 2016;

54 Kirkby et al., 2016; Tröstl et al., 2016) together with H_2O vapour, NH_3 (Kirkby et al., 2011),

55 amines (Almeida et al., 2013), other oxidation products of volatile organic compounds (VOCs;

56 Metzger et al., 2010; Schobesberger et al., 2013; Riccobono et al., 2014) and some inhibiting

57 chemical species (e.g. isoprene or NO_2; Kiendler-Scharr et al., 2009; Kerminen et al., 2018)

58 can play an important role in both the particle formation and growth. The VOCs include

59 compounds of both anthropogenic and biogenic origin, mainly isoprenoids such as α-pinene

60 (Kirkby et al., 2016). In some specific coastal regions, iodine oxides produced from marine

61 biota are involved (O'Dowd et al., 2002). Atmospheric concentration of these key compounds

62 at a level that is smaller by 12–14 orders of magnitude than the concentration of air molecules

63 is already sufficient for the phenomenon (Kulmala et al., 2014). Relative importance of the

64 organics increases with particle size (Riipinen et al., 2011; Ehn et al., 2014), and their

65 supersaturation is maintained by fast gas-phase autooxidation reactions of VOCs (Crounse et

2

66 al., 2013). The overall phenomenon is ordinarily confined in time for 1 day or so, and, therefore,

67 it can be regarded as an event in time, and is referred as new aerosol particle formation (NPF)

68 and consecutive particle diameter growth event.

69

70 Such events appear to take place almost everywhere in the world and anytime (Kulmala et al.,

71 2004; Kerminen et al., 2018; Nieminen et al., 2018). Their occurrence frequency and, more

72 importantly, their contribution to particle number concentrations were found to be substantial

73 or determinant in the global troposphere (Spracklen et al., 2006; Kulmala et al., 2014).

74 Moreover, their contribution to the number of cloud condensation nuclei (CCN) can be 50% or

75 even more (Makkonen et al., 2009; Merikanto et al, 2009; Sihto et al., 2011), which links the

76 events to climate system, and emphasizes their global relevance (Kerminen et al., 2012;

77 Makkonen et al., 2012; Carslaw et al., 2013; Gordon et al., 2016). New particle formation and

78 growth events were proved to be common in polluted air of large cities as well with a typical

79 relative occurrence frequency between 10% and 30% (Woo et al., 2001; Baltensperger et al.,

80 2002; Alam, et al., 2003; Wehner et al., 2004; Salma et al., 2011; Dall'Osto et al., 2013; Xiao

81 et al., 2015; Zhang et al., 2015; Kulmala et al., 2017, Nieminen et al., 2018). The coupling and

82 relationships between regional and urban (sub-regional) NPF were demonstrated at least under

83 favourable orographic conditions (Salma et al., 2016b). New particle formation can increase

84 the existing particle number concentrations in city centres by a factor of approximately 2 on

85 nucleation days, while it can produce 13–28% of ultrafine (UF) particles as a lower estimate on

86 a longer (e.g. annual) time scale (Salma et al., 2017). Particle concentrations from NPF are also

87 important when compared to (primary) particles emitted by their dominant source in cities,

88 namely by road vehicles with internal combustion engines (Paasonen et al., 2016). These results

89 jointly suggest that particles from NPF and growth events in cities can influence not only the

90 urban climate but can contribute to the public's excess health risk from particle number

91 exposures (Oberdörster et al., 2005; Braakhuis et al., 2014; Salma et al., 2015), and,

92 furthermore, could be linked to the role of human actions in all these effects.

93

94 Despite these potentials, conclusive interpretation of the data obtained, and results derived

95 specifically for cities remained hindered so far. Several-year long, semi-continuous, critically

96 evaluated, complex and coherent data sets are required for this purpose, which have been

97 generating gradually. As part of this international progress, investigations dedicated to urban

98 NPF and growth events in Budapest have been going on since November 2008. Measurements

99 for 5 full years were realised in the city centre at a fixed location, 1 full year was devoted to

measurements in a near-city background environment, and some other measurements were accomplished in different urban microenvironments for time intervals of a few months. The main objectives of this study are to determine, present and analyse the dynamic properties, i.e. particle formation rate and particle diameter growth rate, timing properties, i.e. starting time and duration time interval of nucleation process of NPF and growth events together with the major sources and sink of condensing vapours, basic meteorological data and criteria pollutant gases for 6 years, to investigate and interpret their relationships, to discuss their monthly distributions, to evaluate and detect some of their features specific for urban atmospheric environments, and to demonstrate some specific urban influence on the calculation of the properties. These quantities and relationships are of basic importance in many atmospheric processes for several reasons. Our goals are in line with the research needs for global atmospheric nucleation studies (Kerminen et al., 2018; Nieminen et al., 2018).

2 Experimental methods

The measurements took place at two urban locations in Budapest, Hungary. Most measurements were realised at the Budapest platform for Aerosol Research and Training (BpART) facility (N 47° 28' 29.9", E 19° 3' 44.6", 115 m above mean sea level (a.s.l.; Salma et al., 2016a). This site represents a well-mixed, average atmospheric environment for the city centre. The other location was situated at the NW border of Budapest in a wooded area of the Konkoly Astronomical Observatory of the Hungarian Academy of Sciences (N 47° 30' 00.0", E 18° 57' 46.8", 478 m a.s.l.). This site characterises the air masses entering the city since the prevailing wind direction in the area is NW. The measurements were accomplished for 6 full-year long time intervals, i.e. from 03–11–2008 to 02–11–2009, from 19–01–2012 to 18–01–2013, from 13–11–2013 to 12–11–2014, from 13–11–2014 to 12–11–2015, from 13–11–2015 to 12–11–2016 and from 28–01–2017 to 27–01–2018. In the measurement year 2012–2013, the instruments were set up in the near-city background, while in all other years, they were installed in the city centre. Local time (LT=UTC+1 or daylight-saving time, UTC+2) was chosen as the time base of the data unless otherwise indicated because it had been observed in earlier investigations that the daily activity time pattern of inhabitants substantially influences many atmospheric processes in cities (Salma et al., 2014; Sun et al. 2019).

The main measuring system was a flow-switching type differential mobility particle sizer (DMPS). It consists of a radioactive (^{60}Ni) bipolar charger, a Nafion semi-permeable membrane

dryer, a 28-cm long Vienna-type differential mobility analyser and a butanol-based condensation particle counter (TSI, model CPC3775). The sample flow was 2.0 L min^{-1} in the high-flow mode, and 0.31 L min^{-1} in the low-flow mode with sheath air flow rates 10 times larger than for the sample flows. The DMPS measures particle number concentrations in an electrical mobility diameter range from 6 to 1000 nm in the dry state of particles (with a relative humidity of RH<30%) in 30 channels, which finally yields 27 channels after averaging 3 overlapping channels when joining the data for the 2 flow modes. The time resolution of the measurements was approximately 10 min till 18–01–2013, and 8 min from 13–11–2013 (after a planned update of the DMPS system). There was no upper size cut-off inlet applied to the sampling line, and a weather shield and insect net were only attached. The sampling inlets were identical at both locations except for the ~~installed at a~~ height of the installation above the ground, which w~~as~~ ~~of~~ 12.5 m ~~above the street level~~ in the city centre~~,~~ and ~~of~~ approximately 1.7 m in the near-city background. The measurements were performed according to the international technical standard (Wiedensohler et al., 2012). The availability of the DMPS data over 1-year long time intervals are summarised in Table 1.

Synoptic meteorological data for air temperature (T), RH, wind speed (WS) and wind direction (WD) were obtained from a measurement station of the Hungarian Meteorological Service (HMS, station no. 12843) by standardised methods with a time resolution of 1 h. Global solar radiation (GRad) data were measured by the HMS at a distance of 10 km in E direction with a time resolution of 1 h. Meteorological data were available in >90% of the possible cases in each year. Concentrations of SO_2, O_3, NO_x and CO were obtained from measurement stations of the National Air Quality Network in Budapest (in a distance of 4.5 km from the urban site, and of 6.9 km from the near-city background site) located in the upwind prevailing direction from the measurement sites. They are measured by UV fluorescence (Ysselbach 43C), UV absorption (Ysselbach 49C), chemiluminescence (Thermo 42C) and IR absorption methods (Thermo 48i), respectively with a time resolution of 1 h. The concentration data were available in >85% of the yearly time intervals, and >98% of them were above the limit of determinations (LOD). It is worth mentioning that the LOD of the SO_2 analyser was approximately 0.2 µg m^{-3}, and that the hourly average SO_2 concentration ~~of SO_2~~ in the Budapest area is ordinarily distributed without larger spatial gradients (Salma et al., 2011). For the present study, this was proved by evaluating the concentration ratios from 2 different municipal stations which are in the closest distance from the BpART facility in 2 different directions with an angle of 60° between them. The mean SO_2 concentration ratio and standard deviation (SD) for the 2 stations were 81±20%

168   over the 5-year long measurement time interval. The assumption can also be justified indirectly

169   by a conclusion on the monthly distribution of SO_2 concentration in Sect. 4.2.

170

171   **3 Data treatment**

172

173   The measured DMPS data were evaluated according to the procedure protocol recommended

174   by Kulmala et al. (2012) with some refinements that are related to urban features (see Sect. 3.1).

175   Particle number concentrations in the diameter ranges from 6 to 1000 nm (N), from 6 to 25 nm

176   (N_{6-25}), from 6 to 100 nm (N_{6-100} or UF particles) and from 100 to 1000 nm ($N_{100-1000}$) were

177   calculated from the measured and inverted DMPS concentrations. Particle number size

178   distribution surface plots showing jointly the variation in particle diameter and particle number

179   concentration density in time were also derived. Identification and classification of NPF and

180   growth events was accomplished on these surface plots (Dal Maso et al., 2005; Németh et al.,

181   2018) on a daily basis into the following main classes: NPF event days, non-event days, days

182   with undefined character, and days with missing data (for more than 4 h during the midday).

183   Relative occurrence frequency of events was determined for each month and year as the ratio

184   of the number of event days to the total number of relevant (i.e. all−missing) days. A subset of

185   NPF events with uninterrupted evolution in time, which are called quantifiable (class 1A)

186   events, were further separated because the time evolution of their size distribution functions

187   was utilised to determine the dynamic and timing properties with good accuracy and reliability.

188

189   **3.1 Dynamic and timing properties**

190

191   Growth rate (GR) of nucleation-mode particles was calculated by mode-fitting method

192   (Kulmala et al., 2012). Particle number median mobility diameter (NMMD) of the nucleation

193   mode were obtained from fitting the individual size distributions by DoFit algorithm (Hussein

194   et al., 2004). The growth rate was determined as the slope of the linear line fitted to the time

195   series of the NMMD data within a time interval around a diameter d, where the dependency

196   could be satisfactorily approximated by linear fit. Since the nucleation mode was mostly

197   estimated by N_{6-25} in the calculations of the formation rate (see below), and since the median

198   of the related diameter interval (from 6 to 25 nm) is close to d=10 nm, GRs for particles with a

199   diameter of 10 nm were determined (GR_{10}). This type of GR can be interpreted as an average

200   GR as far as the given particle diameter range is concerned, but it actually expresses the

201   beginning of the growth process only. Particle growth can slow substantially in time in specific

202   cases, and this can affect considerably the formation rate calculations (see later).

203

204   Time evolution of an aerosol population is described by the general dynamic equation which

205   was rearranged, simplified and approximated by several quantities (Kulmala et al., 2001; Dal

206   Maso et al., 2002; Kulmala et al., 2012; Cai and Jiang, 2017) to express the formation rate J_6

207   of particles with the smallest detected diameter of d_{min}=6 nm in a form utilised in the present

208   evaluation as

209

210      $$J_6 = \frac{dN_{6\text{-}25}}{dt} - \frac{dN_{Ai,<25}}{dt} + \text{CoagS}_{10}(N_{6\text{-}25} - N_{Ai,<25}) + \frac{\text{GR}_{10}}{(25-6)}(N_{6\text{-}25} - N_{Ai,<25}) . \qquad (1)$$

211

212   The first term on the right side of Eq. 1 expresses the concentration increment. The particle

213   number concentration in the size range from 6 to 25 nm (i.e. $N_{6\text{--}25}$) is usually selected to

214   approximate the nucleation-mode particles $N_{nuc} \approx N_{6\text{--}25}$. This is a reasonable choice because it

215   was proved to be advantageous and effective way in handling fluctuating data sets since $N_{6\text{--}25}$

216   often exhibits smaller scatter in time and less sensitivity than the fitted area of the nucleation

217   mode. It is implicitly assumed that the intensity of the NPF is constant for a certain time interval,

218   and, therefore, $dN_{6\text{--}25}/dt$ can be determined as the slope of the linear function of $N_{6\text{--}25}$ versus

219   time t within an interval where the dependence could be satisfactorily approximated by linear

220   fit. A limitation of the relatively wide size range (6–25 nm) selected can be manifested by

221   disturbances from primary particles particularly in urban environments. This is taken into

222   account by an additional term of $N_{Ai,<25}$, which is discussed below.

223

224   The second term on the right side of Eq. 1 expresses the contribution of high-temperature

225   emission sources, usually of vehicular road traffic (Paasonen et al., 2016; Salma et al., 2017) to

226      $N_{6\text{--}25}$, which can provisionally disturb the assumption of $N_{nuc} \approx N_{6\text{--}25}$. A typical example of such

227   a situation is shown in Fig. S1a from 10:09 to 12:23 LT. In these specific cases, the contribution

228   of primary emissions was estimated from the slope of the time series of the fitted peak area of

229   the Aitken mode below d<25 nm ($N_{Ai,<25}$) in the time region under consideration. Reliable

230   separation of the nucleation and Aitken modes from each other was hindered or was not possible

231   for a few individual size distributions due to overlapping modes and the scatter in the measured

232   concentration data, and these individual cases were excluded from or skipped in the time series.

233

234   The third term on the right side of Eq. 1 represents the loss of particles due to coagulation
235   scavenging (with pre-existing particles). The coagulation scavenging efficiency for particles
236   with a diameter of 10 nm ($CoagS_{10}$) was selected to approximate the mean coagulation
237   efficiency of nucleation-mode particles ($CoagS_{nuc}$). This diameter was chosen by considering
238   the median of the related diameter range, which was discussed above for GR. The coagulation
239   efficiency was calculated from classical aerosol mechanics with adopting a mass
240   accommodation coefficient of 1 and utilizing the Fuchs' transition-regime correction factor
241   (Kulmala et al., 2001; Dal Maso et al., 2005; Kulmala et al., 2013) by using computation scripts
242   developed at the University of Helsinki. Self-coagulation within the nucleation mode was
243   neglected due to limited ambient concentrations. Hygroscopic growth of particles was not
244   considered since this depends on chemical composition of particles, which is unknown.

245

246   The fourth term on the right side of Eq. 1 expresses the growth out of newly formed particles
247   from the ~~considered~~ size range by condensation of vapours. The GR_{10} was selected to
248   approximate a representative value at the median of the particle diameter range considered
249   (Vuollekoski et al., 2012). It is implicitly assumed that GR_{10} can be regarded to be constant
250   over the time interval under consideration. Nevertheless, the growth of nucleation-mode
251   particles in time is occasionally limited (Fig. S1b). In these specific cases, the mean relative
252   area of the nucleation mode below 25 nm was determined by fitting individual size distributions
253   around the time of the maximum nucleation-mode NMMD, and the ratios were averaged. A
254   correction in form of the mean relative area was adopted as a multiplication factor for the
255   growth out term in Eq. 1. On very few days, the growth of newly formed particles was followed
256   by a decrease in nucleation-mode NMMD (Salma et al., 2016a). In these cases, the shrinkage
257   rate (with a formal $GR_{10}<0$) was derived and adopted in Eq. 1. Relative contributions of the
258   concentration increment coagulation loss and growth out from the diameter interval to J_6 are
259   decreasing in this order with mean values of 71%, 17% and 12%, respectively (Table S1).

260

261   The formation and growth rates for the measurement years of 2008–2009 and 2012–2013 were
262   calculated earlier by a slightly different way and neglecting the urban features discussed above
263   (Salma et al., 2011, 2016b). To obtain consistent data sets, the dynamic properties for these 2
264   years were re-evaluated by adopting the present improved protocol and implementing the
265   experience gained over the years. The mean new-to-old rate ratios with SDs for the GR_{10} and
266   J_6 were 1.06±0.32 and 1.23±0.37, respectively in the city centre (2008–2009) and 1.04±0.21
267   and 1.20±0.35, respectively in the near-city background (2012–2013). It was the smaller rates

268 that were primarily and sometimes substantially impacted. The modifications were
269 simultaneously adopted. The subtraction of particle number concentrations emitted by road
270 traffic from N_{6-25}, which usually leads to a decrease in the coagulation loss term and loss term
271 due to growth out from the diameter range of 6–25 nm. At the same time, the subtraction, and
272 which can also influence the slope of the concentration change in time (dN_{nuc}/dt) depending on
273 the actual time evolution of perturbing emission source. In addition to that, the time interval in
274 which this slope is considered to be constant was set in a new treatment. It is noted that the
275 relative contributions of the concentration increment, coagulation loss and growth out from the
276 diameter interval to J_6 have different weights in propagating their effects. Furthermore, J_6 itself
277 also depends on GR_{10}, which makes the relationships even more complex. These connected
278 effects explain why the changes resulted in increments. The re-calculation is considered as a
279 methodological improvement over the years of research.

280

281 The assumptions and estimations above usually represent a reasonable approximation to reality.
282 The N_{6-25} is derived from the experimental data in a straightforward way, the GR_{10} and the
283 corrections for primary particles and limited particle growth depend on the quality of the size
284 distribution fitting as well, while the $CoagS_{10}$ is determined by using a theoretical model. The
285 resulting accuracies of the dynamic properties, in particular of J_6, look rather complicated. They
286 also depend on the spatial heterogeneity in the investigated air masses particularly for the
287 observations performed at the fixed site, size and time resolution of the concentrations
288 measured, diameter range of the size distributions, fluctuations in the experimental data,
289 selection of the particle diameter interval, choice of the time interval of interest (for linear fits),
290 sensitivity of the models to the input uncertainties (Vuollekoski et al., 2012), and also on the
291 extent of the validity of the assumptions applied under highly polluted conditions (Cai and
292 Jiang, 2017). The situation is further complicated with the fact that the dynamic (and also the
293 timing) properties are connected to each other. Finally, it is important to recognise that some
294 NPF and growth curves on the surface plots have rather broad starting time interval (Fig. S1b
295 and S1c). They occur in a considerable abundance in cities, e.g. in 40% of all quantifiable events
296 in Budapest (Sect. 4.4). This may yield badly defined or composite dynamic properties, whose
297 uncertainty can have principle limitations which can prevail on the experimental and model
298 uncertainties.

299

300 Timing properties of NPF and growth events are increasingly recognised, and they can provide
301 valuable information even if they are estimated indirectly from the observed diameter interval

9

302 >1.5 nm (Sect. 1). The earliest estimated time of the beginning of a nucleation (t_1) and the latest

303 estimated time of the beginning of a nucleation (t_2) were derived by a comparative method

304 (Németh and Salma, 2014) based on the variation in the content of the first size channel of the

305 DMPS system. Both time parameters include a time shift that accounts for the particle growth

306 from the stable neutral cluster mode at approximately 2 nm to the smallest detectable diameter

307 limit of the DMPS systems (6 nm in our case) by adopting the GR value in the size window

308 nearest to it in size space. The difference $\Delta t = t_2 - t_1$ is considered as the duration time interval of

309 the nucleation process. It represents the time interval during which new aerosol particles are

310 generated in the air. The timing properties are expressed in UTC+1, and their uncertainty is

311 regarded to be ca. 30 min under ordinary NPF and growth situations.

312

313 **3.2 Sources and sink**

314

315 Relative effects and role of gas-phase H_2SO_4 were estimated by its proximity measure (proxy

316 value) containing both its major source and sink terms under steady-state conditions according

317 to Petäjä et al. (2009). It was calculated for GRad>10 W m^{-2}. Formaly, it is possible to convert

318 the H_2SO_4 proxy values to H_2SO_4 concentrations by an empirical scaling factor of $k=1.4\times10^{-7}\times GRad^{-0.70}$, where GRad is expressed in a unit of W m^{-2} (Petäjä et al., 2009). The factor was,

320 however, derived for a remote boreal site, and, therefore, we prefer not to perform the

321 conversion since urban areas are expected to differ from the boreal regions~~, and adopting the~~

322 ~~factor could distort the dynamic relationships or time trends investigated~~. The conversion was

323 applied only to estimate the order of average H_2SO_4 atmospheric concentration levels. The

324 results derived by utilising the proxy are subject to larger uncertainties than for the other

325 properties because of these limitations, but they may indicate well gross tendencies.

326

327 Condensation sink for vapour molecules onto the surface of existing aerosol particles was

328 computed for discrete size distributions as described in earlier papers (Kulmala et al., 2001; Dal

329 Maso et al., 2002, 2005) and summarised by Kulmala et al. (2013). The equilibrium vapour

330 pressure of the condensing species was assumed to be negligible at the surface of the particles,

331 thus similar to sulfuric acid. Dry particle diameters were considered in the calculations.

332

4 Results and discussion

Annual median total particle number concentrations (*N*) for each measurement year are summarised in Table 1. ~~based on the individual data in the near-city background in 2012–2013, and in the city centre for the separate measurement years of 2008–2009, 2013–2014, 2014–2015, 2015–2016 and 2017–2018 were 3.4×10³, and 11.5×10³, 9.7×10³, 9.3×10³, 7.5×10³ and 10.6×10³ cm⁻³, respectively.~~ The data for the city centre indicate a moderate decreasing trend. ~~The first 4 values unambiguously show a decrease, while the last data point may look somewhat differently. Rigorous statistical evaluation of the joint data set of particle number concentrations in various size fractions over a decennial time interval from November 2008 to November 2018 is in progress, and its preliminary results in the one hand, confirm the decreasing tendency, and in the other hand, reveal some fine structure to this dependency.~~ The mean UF/*N* ratio with SD for the same measurement time intervals were $67\pm14\%$, and $79\pm6\%$, $75\pm10\%$, $75\pm11\%$, $76\pm11\%$ and $80\pm10\%$, respectively. The values correspond to ordinary urban atmospheric environments in Europe (Putaud et al., 2010, Sun et al., 2019).

An overview on the number of classified days for each measurement year~~separately for the 1-year long measurement time intervals~~ is also given in Table 1. The availability of the daily size distribution surface plots with respect to all days ensures that the data are representative on yearly and monthly time scales, except for the months August and September 2015, when there were missing days in larger ratios. The number of quantifiable event days (248 cases) is also considerable, which establishes to arrive at firm conclusion for the NPF and growth events as well.

11

357 **Table 1.** Annual median total particle number concentrations (in 10^3 cm^{-3}), n~~N~~umber of days with ~~new~~
358 ~~aerosol particle formation~~NPF and growth event, quantifiable ~~(class 1A)~~ event days, non-event days,
359 undefined days, missing days and the coverage (in %) of relevant days ~~with respect to all days~~ in the
360 near-city background and city centre separately for the 1-year long measurement time intervals.

361

| Environment	Background	Centre				
Time interval	2012–2013	2008–2009	2013–2014	2014–2015	2015–2016	2017–2018
Concentration	3.4	11.5	9.7	9.3	7.5	8.7
Event days	96	83	72	81	35	83
Quantifiable days	43	31	48	56	18	52
Undefined days	19	34	24	25	8	23
Non-event days	231	229	267	240	226	257
Coverage	95	95	99	95	73	99
Missing days	20	19	2	19	97	2

362

363

364 It was previously shown that the NPF and growth events observed in the city centre of Budapest
365 and its background ordinarily happen above a larger territory or region in the Carpathian Basin
366 (Németh and Salma, 2014), and they are linked to each other as a spatially coherent and joint
367 atmospheric phenomenon (Salma et al., 2016b). From the point of the occurrence frequency
368 distribution, they can, therefore, be evaluated jointly in the first approximation. An overall
369 monthly mean relative occurrence frequency of nucleation days derived for all 6 measurement
370 years is shown in Fig. 1. The annual mean frequency with SD was 22±5%, which is considerable
371 and is in line with other urban sites (Sect. 1). The monthly mean frequency has a temporal
372 variation, which can be characterised by a noteworthy pattern. The mean monthly dependency
373 exhibits an absolute and a local minimum in January (5.6%) and August (21%), respectively,
374 and an absolute and a local maximum in April (40%), and September (31%), respectively.
375 Nevertheless, the SDs of the monthly means indicate prominent variability from year to year.
376 The pattern can be related to multivariate relationships and complex interplay among the
377 influencing factors, which include the air temperature (January is the coldest month, while
378 August is the warmest month in the Carpathian Basin) and enhanced emission of biogenic
379 VOCs in springtime (March–April) and early autumn (September) as well (Salma et al., 2016b).
380 It is noted that the findings derived for the separate city-centre data set are very similar to the
381 results presented above.

382
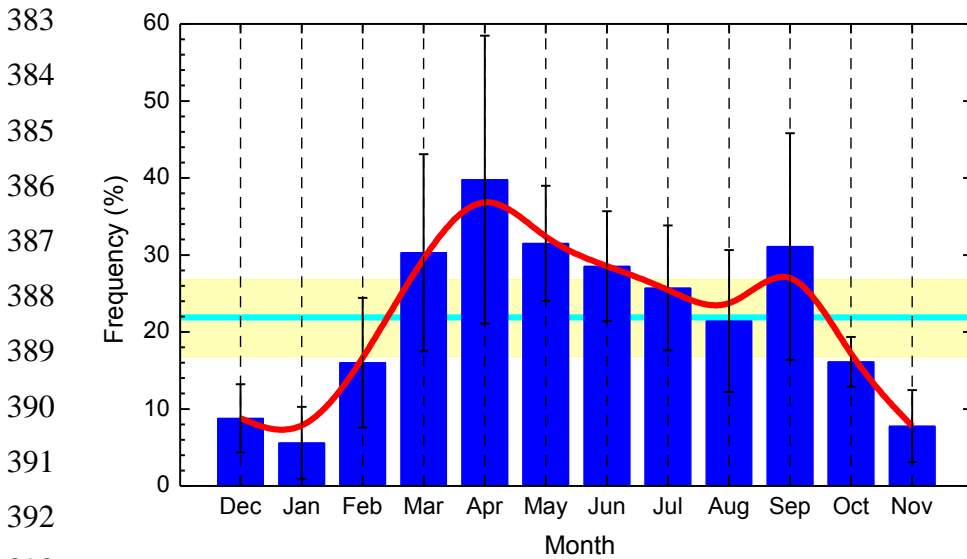
Figure 1. Monthly mean relative occurrence frequency of ~~new aerosol particle formation~~NPF and ~~consecutive particle diameter~~ growth events ~~with respect to the number of relevant days~~ for the joint 6-year long data set. The error bars show ±1 standard deviation, the horizontal line in cyan indicates the overall annual mean frequency, the yellow bands represent ±1 standard deviation of the annual mean, and the smooth curve in red serves to guide the eye.

The properties and variables studied were derived in full time resolution. They were averaged in several ways for different conditions and for various purposes to obtain typical average descriptive characteristics. In 1 case (31–08–2016), the NPF and growth event could reliable be identified, while the measured absolute particle number concentrations could not be validated due to ~~some~~ experimental troubles, and, therefore, it was left out from the further calculations. Similarly, there were 1 and 4 events with unusually/extraordinarily large dynamic properties in the measurement years 2014–2015 and 2017–2018, respectively. More specifically, 5 individual J_6 data when expressed in a unit of cm^{-3} s^{-1} and 1 individual GR$_{10}$ data when given in nm h^{-1} were >20 (Table 3). These extremes were left out from the overview statistics to maintain the representativity (they could be influenced by some unknown extra or very local sources) and to fulfil better the basic requirements of correlation analysis. If an event showed a double beginning then the dynamic properties for the first onset were considered in the basic overview since this onset is of regional relevance (Salma et al., 2016b). The extreme NPF and growth events and the characteristics for the second onsets were, however, evaluated separately and are discussed in detail and interpreted in Sect. 4.4.

4.1 Ranges and averages

Ranges and averages with SDs of formation rate J_6, growth rate GR_{10}, starting time of nucleation (t_1) and duration time interval of nucleation (Δt) are summarised in Table 2 for separate measurement years and for the joint 5-year long city centre data set. In the city centre, nucleation generally starts at 09:15 UTC+1, and it is typically maintained for approximately 3 h. The NPF and growth events ordinarily produce 5.6 new aerosol particles with a diameter of 6 nm in 1 cm^3 of air in 1 s, and cause the particles with a diameter of 10 nm to grow with a typical rate of 7.6 nm h^{-1}. The statistics for J_6 and GR_{10} are based on 199 and 203 events, respectively. The corresponding data for the separate years show considerable variability without obvious trends or tendencies. The differences between the years can likely be related to changes in actual atmospheric chemical and physical situations and conditions, and to the resulting modifications in the sensitive balance and delicate coupling among them from year to year. Spread of the individual data for GR_{10} is smaller than for J_6; the relative SDs for the joint 5-year long city centre data set were 38% and 68%, respectively, while the (external) relative SDs calculated from the annual mean values were 4.2% and 14.0%, respectively.

The dynamic properties and t_1 data tend to be smaller in the near-city background than in the city centre. In general, nucleation starts 1 h earlier in the background, and the events typically show significantly smaller J_6 (with a median of 2.0 cm^{-3} s^{-1}) and GR_{10} (with a median of 5.0 nm h^{-1}). Duration of the nucleation is very similar to that in the city centre. All starting times of nucleation were larger than (in a few cases, very close to) the time of the sunrise. This implies that no nocturnal NPF and growth event has been identified in Budapest so far. The particle growth process (the so-called banana curve) could be traced usually for a longer time interval (up to 1.5 d) in the background than in the centre.

These results are in line with the ideas on atmospheric nucleation and consecutive particle growth process (e.g. Kulmala et al., 2014; Zhang et al., 2015; Kerminen et al., 2018). It was observed in a recent overview study (Nieminen et al., 2018) that the formation rate of 10–25 nm particles increased with the extent of anthropogenic influence, and in general, it was 1–2 orders of magnitude larger in cities than at sites in remote and clean environments. This highlights the importance of some anthropogenic vapours such as SO_2, NH_3 and amines to NPF and growth. The data also confirm our earlier findings with respect to Budapest and its regional

14

451

452 **Table 2.** Ranges, averages and standard deviations of aerosol particle formation rate J_6, particle diameter

453 growth rate GR_{10}, starting time (t_1) and duration time interval ($\Delta t=t_2–t_1$) of nucleation process of

454 quantifiable ~~(class 1A) new particle formation~~NPF and growth events in the near-city background and

455 city centre separately for the 1-year long measurement time intervals and for the joint 5-year long city

456 centre data set.

457

Environment	Background	Centre					
Time interval	2012–2013	2008–2009	2013–2014	2014–2015	2015–2016	2017–2018	All 5 years
Formation rate J_6 (cm^{-3} s^{-1})							
Minimum	0.48	1.47	1.13	0.81	1.19	1.60	0.81
Median	2.0	4.2	3.5	4.4	4.6	6.3	4.6
Maximum	5.6	15.9	17.8	18.0	15.3	17.3	18.0
Mean	2.2	4.7	5.2	5.6	5.0	6.6	5.6
St. deviation	1.3	2.6	3.7	4.2	3.7	3.3	3.8
Growth rate GR_{10} (nm h^{-1})							
Minimum	3.0	3.7	3.1	2.8	3.2	3.3	2.8
Median	5.0	7.6	6.6	6.5	8.0	7.5	7.3
Maximum	9.8	17.4	19.0	18.0	15.5	19.8	19.8
Mean	5.2	7.8	7.2	7.3	7.7	8.0	7.6
St. deviation	1.4	2.6	2.8	3.2	3.0	2.8	2.9
Starting time, t_1 (HH:mm UTC+1)							
Minimum	05:51	07:14	06:44	05:48	07:31	05:57	05:48
Median	08:19	09:26	09:22	08:48	09:45	09:18	09:15
Maximum	11:09	11:38	12:21	11:23	12:45	12:15	12:45
Mean	08:17	09:27	09:25	08:49	10:02	09:24	09:19
St. deviation	01:11	01:05	01:26	01:22	01:23	01:36	01:26
Duration time, Δt (HH:mm)							
Minimum	01:23	00:52	00:42	00:31	01:03	01:26	00:31
Median	03:16	02:36	02:04	03:53	02:31	03:49	02:57
Maximum	06:44	06:04	05:34	07:46	06:05	07:55	07:55
Mean	03:30	02:44	02:14	03:52	02:58	03:57	03:18
St. deviation	01:40	01:11	01:01	01:40	01:47	01:39	01:40

458

459 Ranges and averages with SDs of some related atmospheric properties, namely of mean CS

460 averaged for the time interval from t_1 to t_2, daily maximum gas-phase H_2SO_4 proxy, daily mean

461 T and RH (Table S2), and of daily median concentrations of SO_2 (as the major precursor of gas-

462 phase H_2SO_4), O_3 (as an indicator of photochemical activity), NO_x and CO gases (as indicators

463 of anthropogenic combustion activities and road vehicle emissions) (Table S3) were also

464 derived for quantifiable NPF and growth event days, and are further evaluated. The annual

465 mean CS values exhibited decreasing tendency in the city centre over the years (as can be

466 expected from the particle number concentrations as well). The individual values remained

467 below approximately 20×10^{-3} s^{-1}, which agrees well with the results of our earlier study (Salma

468 et al., 2016b) according to which the CS suppresses NPF above this level in the Carpathian

469 Basin. Maximum H_2SO_4 proxy values reached substantially higher levels (by a factor of

470 approximately 2) in the near-city background than in the city centre due mainly to the

471 differences in the CS and [SO_2]. The differences between the 2 sites are particularly evident

472 when considering their smallest values. The largest variability in the annual average values

473 were observed for the proxy. Median concentration of H_2SO_4 molecules was roughly estimated

474 to be approximately 5×10^5 cm^{-3} by adopting the scaling factor (Sect. 3.2). The air T displayed

475 quite similar and comparable values over the years at both sites. The discussion of its overall

476 effect on the dynamic properties is accomplished in Sec. 4.2, where the monthly distributions

477 are presented. Some events happened at daily mean temperatures below zero. The daily mean

478 RH and its SD for the city centre and near-city background were 54±11% and 64±12%,

479 respectively. There were events that occurred at RHs as high as 90%. Relationships of the

480 dynamic properties with T and RH are also obscured with strong seasonal cycle of these

481 meteorological data and with the fact that air masses arriving to the receptor site in different

482 trajectories are often characterised by distinct levels of meteorological data.

483

484 As far as the pollutant gases are concerned (Table S3), SO_2 showed somewhat smaller daily

485 median values, and O_3 exhibited substantially smaller levels on event days in the city centre

486 than in the near-city background, while concentrations of NO_x and CO were obviously larger

487 in the city than in its close background. The differences can primarily be explained by the

488 intensity and spatial distribution of their major sources and atmospheric chemical reactions, and

489 the joined concentration data resembles typical situations without photochemical smog

490 episodes in cities. There was no obvious decrease in SO_2 concentration during these years in

491 contrast with an earlier decreasing trend from mid-1980s till about 2000.

492

4.2 Monthly distributions

Distributions of the monthly mean J_6, GR_{10}, daily maximum gas-phase H_2SO_4 proxy, mean CS, daily mean air T and RH, and daily median SO_2, O_3, NO_x and CO concentrations for quantifiable NPF and growth events for the joint ~~5-year long~~ city centre data sets are shown in Fig. 2. The distributions – eminently for J_6, GR_{10}, H_2SO_4 proxy and SO_2 – do not follow the monthly pattern of the event occurrence frequency at all (cf. Fig. 1). Instead, the J_6, GR_{10} and H_2SO_4 proxy tend to exhibit larger values in summer months, and they temporal changes over the other months are smooth and do not show distinctive features. The elevations are substantial; the estimated maximum level was larger than the baseline by a factor of 2.1 for the J_6, and by a factor of approximately 1.4 for the GR_{10} and H_2SO_4 proxy. ~~The i~~Intensity of solar radiation ~~at the surface~~, its seasonal cycling, concentration of atmospheric precursors in different months, biogenic processes, anthropogenic activities and the fact that rate coefficients of many thermal chemical/physicochemical processes in the nature (including GR, Paasonen et al., 2018) increase with T could play an important role in explained the distributions. ~~A more comprehensive study involving chemicals and their photochemistry is required for more detailed explanation.~~

~~It is worth mentioning that [SO2] did not change substantially for the NPF event and non-event days, while GRad was typically larger by a factor of ca. 2 and CS was smaller by approximately 30% on event days than on non-event days.~~ The differences in the GRad (and some other properties) are, however, biased by the seasonal cycle of solar electromagnetic radiation via the seasonal variation of NPF occurrence frequency~~, while the CS indicated a modest seasonal dependency. Interpretation of their joint effect should be approached by care, requires further evaluations and is to be realised fully in a further study~~. Nevertheless, the misalignment among the monthly distributions of NPF and growth event occurrence frequency and all the other properties indicates that the occurrence or its basic causes are not linked with the dynamic properties in a straightforward or linear manner in the Carpathian Basin including Budapest.

Some of our results are in line with other observations according to which GR exhibited almost exclusively a summer maximum, while some other finding are different in the sense that the seasonal variability in particle formation rate was quite modest and could not be established earlier (Nieminen et al., 2018). There is one more aspect which may be worth realising in this respect. A large fraction of compounds contributing to NPF and growth in cities can originate

527 from anthropogenic precursors (Vakkari et al., 2015). Their emissions may peak any time of
528 year depending on human habits and requirements (Nieminen et al., 2018). Nevertheless, the
529 fact that our monthly distributions of the dynamic properties in urban environments follow the
530 universal summer maximum behaviour may indicate the overall prevailing role of atmospheric
531 photochemistry coupled with biogenic emissions of aerosol precursor vapours.

532

533 The monthly mean J_6, GR_{10} and H_2SO_4 proxy data still have considerable uncertainty, which
534 makes their interpretation not yet completely conclusive. The uncertainties are influenced by
535 inherent fluctuations in the primary data sets, enhancing effects caused by combining some
536 individual primary data into compound variables (such as H_2SO_4 proxy), number of data items
537 available for different properties and months, variations in other or unknown relevant
538 environmental conditions, and by the variability in relative nucleation occurrence frequency
539 from year to year. The resulting uncertainties are expected to decrease with the length of the
540 available data sets, which emphasized the need to continue the measurements.

541

542 The monthly distributions of CS, and SO_2 and NO_x concentrations could be represented by
543 constant values of the overall means and SDs of $(9.4\pm4.3)\times10^{-3}$ s^{-1}, 4.7±2.1 μg m^{-3} and 81±38
544 μg m^{-3}, respectively with an acceptable accuracy. This suggests that these variables in Budapest
545 do not critically or substantially affect ~~either~~ the dynamic properties (or the event occurrence).
546 Monthly distributions of air T and O_3 concentration showed a maximum over summer months,
547 while RH reflected the T tendency. In addition, monthly averages of T on event days and on
548 non-event days were similar. Both higher biogenic emissions and typically stronger
549 photochemistry are expected during the summer, which enhance the production rate of
550 nucleating and condensing vapours, while there is practically nothing extra in the first
551 approximation (except for extreme Ts) that would suppress the dynamical properties (Kerminen
552 et al., 2018). As result of these complex effects, the dynamic rates showed a summer maximum.
553 This is consistent with the results from other urban and non-urban studies (Nieminen et al.,
554 2018). Distribution of CO was more changing and without obvious tendentious temporal
555 structure or feature than for the other gases, and, therefore, its interpretation is encumbered so
556 far. However, it doesn't seem to substantially affect the dynamic properties.

557
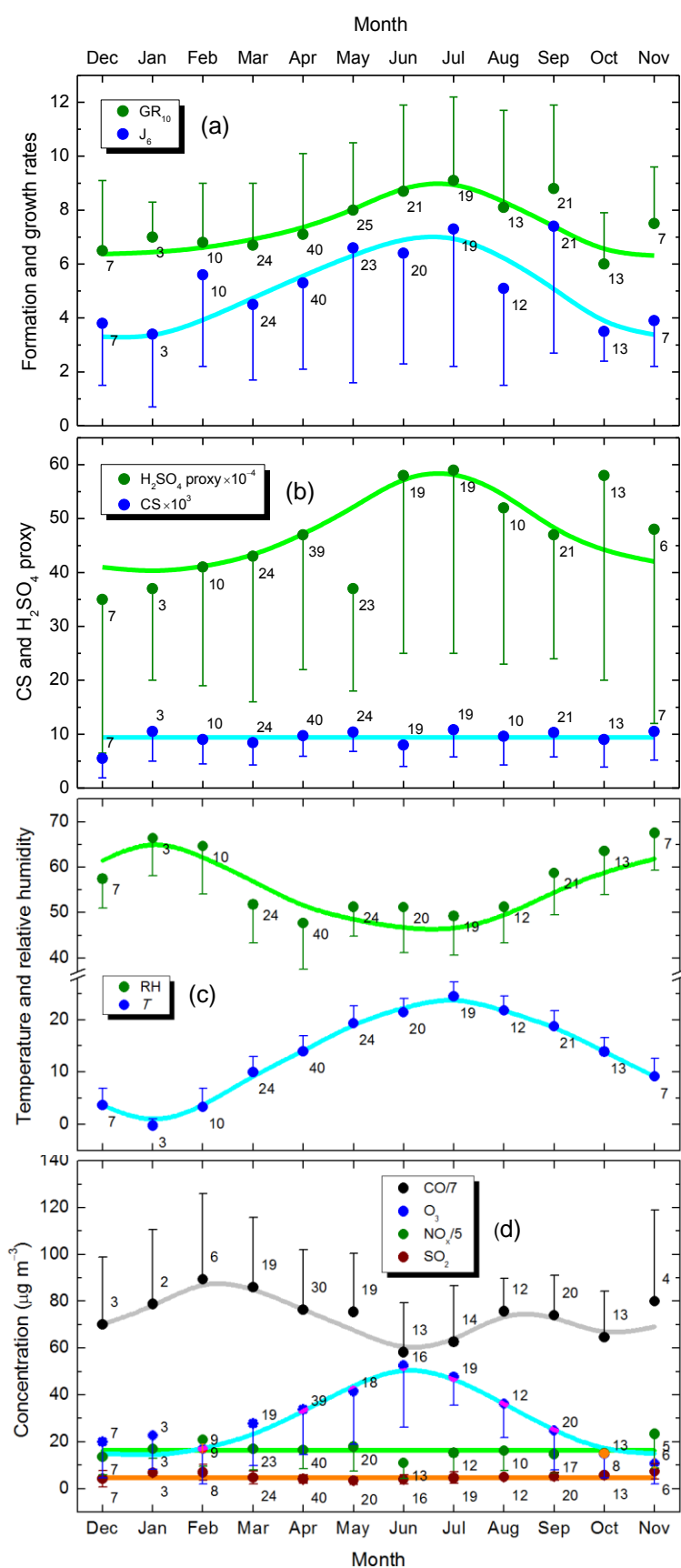
Figure 2. Distribution of monthly mean aerosol particle formation rate J_6 in a unit of cm^{-3} s^{-1} and particle diameter growth rate GR_{10} in a unit of nm h^{-1} (a), mean condensation sink for vapours (CS) in a unit of s^{-1} averaged over the nucleation time interval (t_1, t_2) and daily maximum gas-phase H_2SO_4 proxy in a unit of μg m^{-5} W s (b), daily mean air temperature (T) in a unit of °C and daily mean relative humidity (RH) in % (c), and daily median concentrations of SO_2, O_3, NO_x and CO for quantifiable ~~(class 1A) new particle formation~~NPF and growth events in the city centre for the joint 5-year long time interval. The error bars are shown for one side ~~for clarity~~ and indicate 1 standard deviation. Number of the individual data averaged in each month is displayed next to the symbols. The horizontal lines indicate the overall mean. The nonlinear curves assist to guide the eye.

Distributions of monthly mean ratios of major variables on NPF event days to that on non-event days for the joint city centre data set are summarised in Fig. 3. It is noted that the differences in the number of non-event days and event days are the largest in winter and smallest in spring (Fig. 1). The annual mean ratios for N_{6-100}, GRad, SO_2 and O_3 were above unity, for $N_{100-1000}$ and RH, they were below unity, while the value of CS, NO_x and CO were close to each other on both types of days. Ultrafine particles are generated by NPF and growth processes in a considerable amount; their concentration was larger by 23% on event days than on non-event days. This agrees with our earlier assessment of the NPF contribution as a single source of particles based on nucleation strength factor NSF_{GEN} of 13% as a lower estimate (Salma et al., 2017). The other variables of the first group above represent conditions which favour atmospheric nucleation and particle growth, i.e., strong solar radiation, precursor gas and general photochemical activity, respectively. Particles in the size range of 100–1000 nm (the pre-existing particles with a relatively long residence time) express a condensation and scavenging sink, which represents a competing process to nucleation. There is also evidence that RH acts against continental NPF process (Hamed et al., 2011).

It is also seen in Fig. 3 that NPF and growth events in winter took place preferably when $N_{100-1000}$, CS, RH, NO_x, and CO concentrations were especially low and O_3 concentration was unusually large. It can be explained by considering that the basic preconditions of NPF events are realised by the ratio of source and sink terms for condensing vapours. The source strength in winter is often decreased substantially in the Budapest area (Salma et al., 2017) due to lower solar radiation and less (biogenic) chemical precursors in the air. Nevertheless, NPF can still occur if the sink becomes even smaller. This also explains the lower event day-to-non-event day ratios for N_{6-100} observed in winter months. Full exploitation of the data base by multistatistical and other methods has been in progress and is to be published in a separate article.
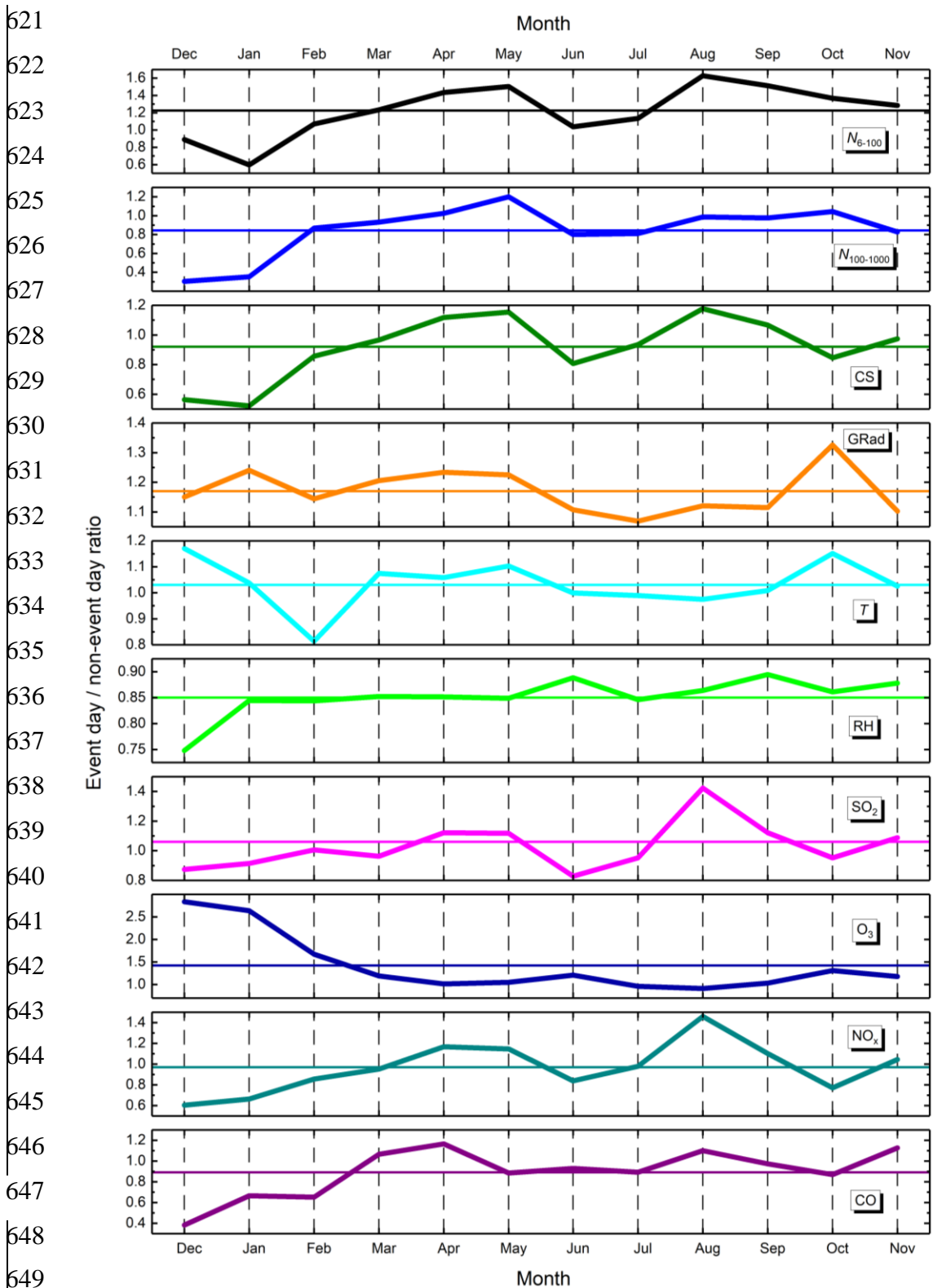
Figure 3. Distributions of monthly mean ratios of median concentrations of N_{6-100}, $N_{100-1000}$, SO_2, O_3, NO_x and CO, and of mean condensation sink for vapours (CS), global solar radiation (GRad), air temperature (T) and relative humidity (RH) on NPF event days to that on non-event days in the city centre for the joint 5-year long time interval. The horizontal lines represent annual average ratios.

4.3 Relationships

Pearson's coefficients of correlation (R) between J_6 and GR_{10} revealed significant linear relationship between them for all annual data sets (the mean R and SD were 0.768±0.099, number of data pairs n=243). This confirms that formation of new aerosol particle and their growth to larger sizes ~~in the atmosphere~~ are tightly and positively linked together. It should be noted that J_6 and GR_{10} are not completely independent variables (see Eq. 1 and Table S1). The linear relationship between the dynamic properties was observed under different atmospheric conditions in many environments (Nieminen et al., 2018). ~~At some sites, this relationship could not be proved due to the weak variability in the variables.~~

The dynamic properties can also be coupled to the concentrations of aerosol precursor compounds and properties of a pre-existing particle population, thus to atmospheric environment (Kerminen et al., 2018). It is, therefore, sensible to investigate the city centre and near-city background data separately. Scatter plots between J_6 and GR_{10} for the 1-year long measurement time intervals are shown in Fig. ~~3~~4. For the city centre, the regression lines follow the line with a slope of 1 in all 5 years. The mean slope (b) with SD for the joint 5-year long city centre data set was b=0.94±0.07 expressed formally in a unit of cm^{-3} s^{-1} nm^{-1} h. At the same time, the regression line for the near-city background deviated significantly with a b=0.67±0.10 cm^{-3} s^{-1} nm^{-1} h from the J_6 vs. GR_{10} dependency for the city centre. This can imply that NPF and growth processes advance in a different manner in these 2 environments. This is likely related to the differences between the city and its close environment as far as the atmospheric composition (for instance, the VOC and NO_x concentrations), chemistry and physics, and other delicate conditions are concerned (Paasonen et al., 2018). The narrower range and smaller number of individual dynamic properties available for the near-city background relative to those in the city centre represent some inherent limitation or weakness in the explanation, and, therefore, it can strictly be regarded as a working hypothesis ~~because a rigorous statistical treatment would require larger variability in the near-city background data~~.

22
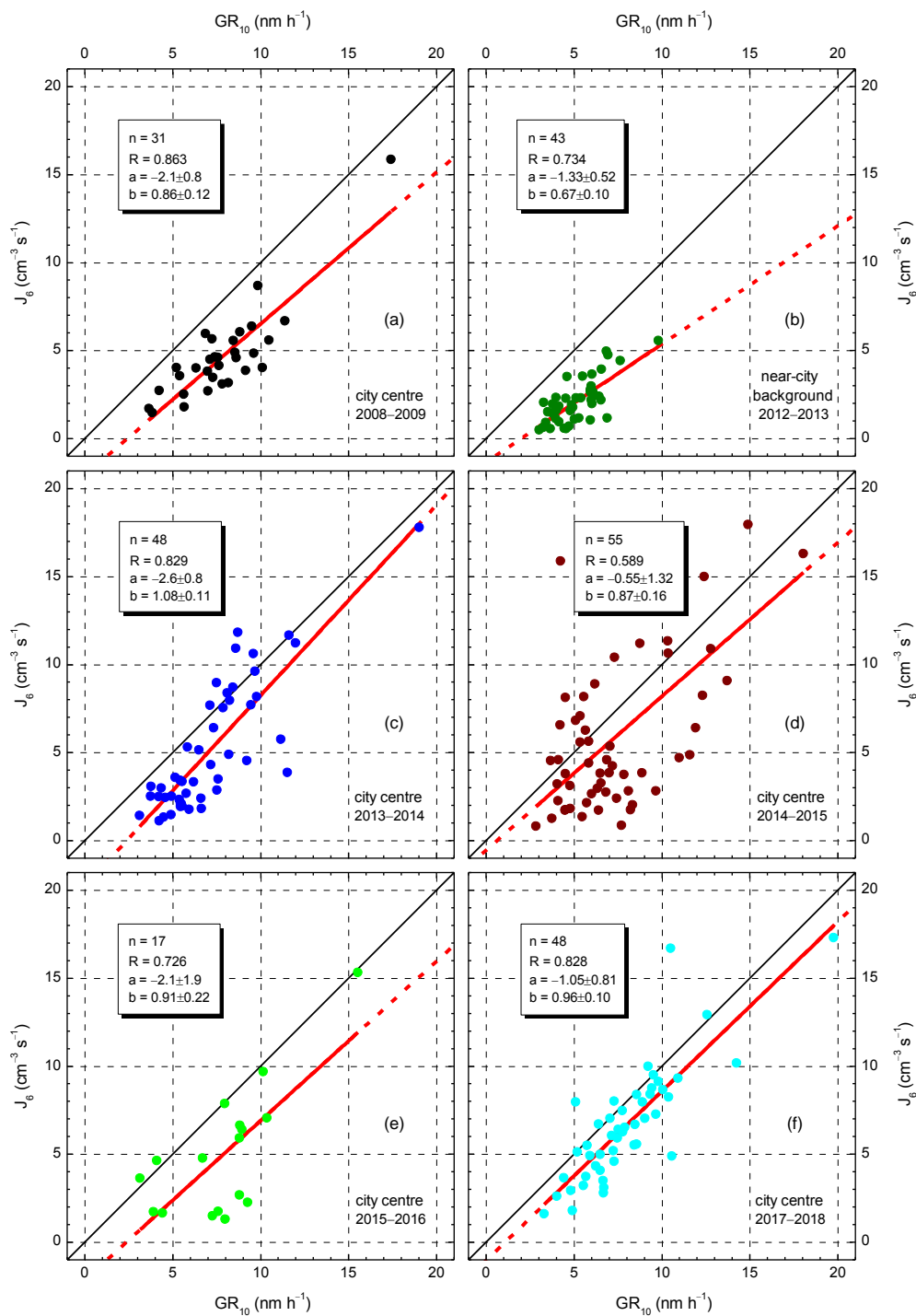
Figure 3~~4~~. Scatter plots for aerosol particle formation rate J_6 and ~~consecutive~~ particle diameter growth rate GR_{10} in city centre (a and c–f) and near-city background (b) separately for the 1-year long measurement time intervals. Number of data point (n), their coefficient of correlation (R) and the intercept (a) and slope (b) of the regression line with standard deviations are also indicated. The lines in black represent the line with a slope of 1, the solid lines in red show the regression lines, while the dashed parts in red are extrapolated from the regression line.

716

The intercepts (*a*) of the regression lines were identical for all data sets within their uncertainty interval. The mean intercept and SD were estimated to be -1.7 ± 0.8 cm^{-3} s^{-1}. This finding is interpreted as the existence of a minimum GR or more exactly of a minimally required GR that leads to $J_6>0$. Particles that exhibit at least this level of GR can escape coagulation mainly with larger particles and reach the detectable diameter (6 nm in our case) by condensational growth. The minimal GR was derived as $GR_{min}=-a/b$, and its mean and SD are 1.8 ± 1.0 nm h^{-1} for the conditions ordinarily present in the Budapest air. Nucleation processes which are initiated under circumstances that cause the newly formed particle with a diameter of 10 nm to grow with a rate $<GR_{min}$ are normally not observed. Anyway, these are expected to be events with relatively small J_6 (weak phenomena) due to the relationship between GR_{10} and J_6. The events with GR larger but close to this limit could be still masked by fluctuating experimental data. Their identification and evaluation can be made feasible by decreasing the lower measurement diameter limit of DMPS systems down to 3 nm, or by different instruments such as particle size magnifier or neutral cluster and air ions spectrometer.

731

Correlations between individual H$_2$SO$_4$ proxy values on one side and J_6 or GR_{10} on the other side were not significant. This is consistent with the corresponding conclusion of Sect. 4.2 and with the earlier results according to which the mean contribution of H$_2$SO$_4$ condensation to the particle GR_{10} was only 12.3% in Budapest (Salma et al., 2016b). The lack of correlation and the average concentrations of SO$_2$ derived separately for ~~the NPF and growth~~ event and non-event days suggest that this precursor gas is ordinarily available in excess and, therefore, it is usually not the lack of SO$_2$ gas itself, which limits the NPF and growth events in Budapest. Instead, the reaction rate of oxidation of SO$_2$ to H$_2$SO$_4$ in the gas phase ~~the formation of H$_2$SO$_4$ is~~ likely governed by photochemical conditions -, and ~~that~~ other chemical species than H$_2$SO$_4$ can have larger influence on the particle growth. The role of H$_2$SO$_4$ in the nucleation process and early particle growth is still determinant or relevant.

743

Coefficients of correlation between CS on one side and J_6 or GR_{10} on the other side for the joint city centre data sets were modest (R=0.41 and 0.32, respectively with n=194 and 197, respectively). This is simply related to the fact that larger GR values are typical for polluted urban air (Kulmala et al., 2017) since particles capable of escaping coagulation scavenging need to grow faster in comparison to cleaner environments, and the enhanced requirements for the growth are linked to increased formation rates as well. It should be noted here that the GR of

750 newly formed particles to larger sizes is primarily coupled to 1) CS, which is further linked to

751 the entire aerosol particle population (including the newly formed particles, thus the NPF itself),

752 2) to the total concentration and some physicochemical properties of non-volatile gaseous

753 compounds and 3) to their production rate in the gas phase from aerosol precursor compounds

754 (e.g. Kerminen et al., 2018). These couplings could result in rather complex behaviour, and

755 their understanding is essential when analysing atmospheric observations.

756

757 As far as the pollutant gases are concerned, no correlation could be identified between J_6 or

758 GR_{10} on one side and the gas concentrations on the other side. The coefficients of correlation

759 between CS and NO_x or CO were modest (R=0.37 and 0.42, respectively with n=164 and 152,

760 respectively), while correlation of NO_x and CO on one side with WS was also modest but

761 negative (R=–0.32 and –0.42, respectively with n=167 and 155, respectively). The former

762 relationships can be explained by the fact that vehicular road traffic in cities is a considerable

763 and common source of NO_x, CO and primary particles (Paasonen et al., 2016), and the emitted

764 particles largely contribute to CS levels. The latter relationships are linked to the effect of large-

765 scale air mass transport (often connected to high WSs) on urban air pollution or air quality.

766

767 **4.4 Extreme and multiple events**

768

769 The data sets of J_6, GR_{10} and Δt containing all, 247 individual values each could be

770 characterised by lognormal distribution function. This is demonstrated by log-probability graph

771 for J_6 in Fig. S2 as example. The coefficient of determination, median and geometric standard

772 deviation for J_6, GR_{10} and Δt data sets were 0.990, 4.0 cm^{-3} and 2.3; 0.993, 6.8 nm h^{-1} and 1.46;

773 and 0.998, 02:57 (0.123 d) and 1.74, respectively. It is noted that the findings derived for the

774 separate city centre data set are very similar to the results presented above.

775

776 One of the major properties of this distribution type is that it contains relatively large individual

777 data with considerably high abundances. There were 5 individual J_6 and 5 individual GR_{10} data

778 above the 98% percentile of the data sets, which belonged to 9 separate NPF and growth events

779 (days). Their specifications, properties and parameters are summarised in Table 3. All these

780 events occurred in the city centre from April to September. The medians of J_6, GR_{10}, CS and

781 air T for the subsets of these 9 extreme event days were larger by factors of 5.2, 2.4, 1.5 and

782 1.4, respectively than for the city centre data. At the same time, the medians of the other

783 atmospheric properties and concentrations in these 2 respective data sets agreed within

approximately 10%. There was a single event associated with an extreme H_2SO_4 proxy (of 23×10^5 µg m^{-5} W s) and relatively low NO_x concentration (44 µg m^{-3}), which indicate exceptionally favourable conditions for NPF and growth. In addition to this case, there were only a few days that were characterised by an unusually large CS (23×10^{-3} s^{-1}) – which could in turn be linked to higher dynamic rates (Sect. 4.3) – or by somewhat larger SO_2 (8.1 µg m^{-3}) or lower NO_x concentration (34 µg m^{-3}). For all the other events, however, no simple or compound property of the investigated variables could explain the extreme rates. Instead, they may be related to some other chemical species and/or atmospheric processes, which were not including in the present study.

Table 3. Date (in a format of dd–MM–yyyy), new particle formation rate J_6 (in a unit of cm^{-3} s^{-1}), particle diameter growth rate GR_{10} (nm h^{-1}), starting time t_1 of nucleation (HH:mm UTC+1), duration time interval $\Delta t = t_2 - t_1$ of nucleation (HH:mm), mean condensation sink CS during the nucleation process (10^{-3} s^{-1}), daily maximum gas-phase H_2SO_4 proxy (10^4 µg m^{-5} W s), daily mean air temperature T (°C), daily mean relative humidity RH (%), daily median concentrations of SO_2, O_3, NO_x (µg m^{-3}) and CO (mg m^{-3}) gases, and the type of the onset for extreme quantifiable ~~(class 1A) new particle formation~~NPF and growth events. The cells in yellow indicate the values which are above the 98% percentile of the corresponding data sets. N.a.: not available.

Date/property	15–09–2009	20–04–2014	19–05–2015	04–07–2015	28–05–2017	25–06–2017	02–08–2017	31–08–2017	09–09–2017
J_6	15.9	17.8	24	16.3	27	33	30	47	17.3
GR_{10}	17.4	19.0	12.2	18.0	9.2	17.0	11.8	21	19.8
t_1	10:20	08:52	08:52	09:38	06:34	10:18	07:39	10:06	11:38
Δt	01:23	01:42	03:57	02:06	07:15	02:46	06:58	06:19	02:06
Proxy	38	42	25	16	229	41	69	92	45
CS	13.4	8.9	13.7	11.9	6.9	10.5	23	18.2	15.5
T	20	13.0	22	26	20	24	29	23	19.1
RH	60	62	48	40	40	68	49	47	58
SO_2	6.1	2.5	4.4	2.3	3.4	3.1	5.6	8.1	6.6
O_3	16.3	43	n.a.	33	61	56	34	24	12.9
NO_x	69	34	174	70	44	66	n.a.	109	112
CO	0.42	n.a.	0.71	0.33	0.31	0.50	0.97	0.62	0.71
Onset	ordinary	double	broad	ordinary	broad	broad	broad	broad	ordinary

805   Each quantifiable NPF and growth event was labelled as ordinary or broad by visual inspection

806   of its beginning part. If the width of the beginning was smaller than approximately 2 h or there

807   was a determinant single growth curve (rib) on the size distribution surface plot then the onset

808   was labelled as ordinary, otherwise as broad (Fig. S1b and S1c for broad onsets). Broad onsets

809   can be generated by 1) long-lasting nucleation process, 2) disrupted and started over nucleation

810   due to changing atmospheric and meteorological conditions or 3) multiple nucleation processes

811   close to each other in time (Salma et al., 2016b). The broad onsets were specified as doublets

812   if the nucleation mode could be separated into 2 submodes by size distribution fitting.

813   Approximately 40% of all quantifiable events had a broad onset. This indicates that ~~NPF and~~

814   ~~growth~~ events with broad/multiple onsets are abundant in the urban environment, which could

815   be an important difference from remote or clean atmospheres.

816

817   For ca. 10% of all quantifiable event days, it was feasible to calculate 2 sets of dynamic

818   properties for onsets 1 and 2 with a reasonable accuracy. In the near-city background, the

819   medians of J_6 and GR_{10} for the onset 1 were similar to the corresponding medians for the whole

820   near-city background data set, while for the onset 2, they were substantially larger, namely 4.1

821   cm^{-3} s^{-1} and 10.0 nm h^{-1}, respectively (cf. Table 2). Actually, the latter values were closer to

822   the medians of the city centre than for the near-city background. Approximately 75% of the

823   doublets resulted in individual onset2/onset1 ratios larger than unity. Their overall median

824   ratios for J_6 and GR_{10} were similar and approximately 1.2, while for the near-city background,

825   they were about 2. The results are in line with our earlier conclusion according to which the

826   second onsets (if it is a new formation process and not just a started over event) are more

827   intensive than the first onsets (Salma et al., 2016b). These particles also grow faster. This can

828   be explained by the fact that the first event is of regional scale since its dynamic properties

829   resemble those of the regional background (Yli-Juuti et al., 2009), while the later event can be

830   characterised by values typical for the city centre (Salma et al., 2016b). The later event (or

831   events) are mainly caused and governed by sub-regional processes. These findings are also

832   coherent with a previous observation of NPF and growth events with multiple onsets in semi-

833   clean savannah and industrial environments (Hirsikko et al., 2013), and they also fit well into

834   the existing ideas on mixing regional and urban air parcels that exhibit different properties such

835   as precursor concentrations, T and RH (Kulmala et al., 2017).

836

5 Conclusions

Magnitude of the particle number concentration level produced solely by NPF and growth ~~(strength of the events)~~ can roughly be estimated by considering the median J_6, median duration of nucleation Δt (their distribution function is lognormal; Table 2) and the mean coagulation loss of these particles F_{coag} (0.17; Sect. 3.1 and Table S1) as: $J_6 \times \Delta t \times (1 - F_{coag})$. In central Budapest, it yields a concentration of 10^4 cm^{-3}. This is in line with another result achieved by nucleation strength factor (Salma et al., 2017). More importantly, the estimated concentration ~~from NPF and growth process~~ is comparable to the annual median atmospheric concentrations (Table 1~~Sect. 4~~). This simple example indicates that the phenomenon is ~~not only~~ relevant not only for aerosol load and climate issues on regional or global spatial scales, ~~—~~which were first recognised. ~~— but i~~It is sensible also to study the ~~can ac~~effects of NPF and growth events on ~~the~~ urban climate and ~~the~~ health risk for inhabitants ~~as well~~ since they produce a large fraction of particles even in cities.

Similar recognitions have led to emerge of urban atmospheric nucleation studies. As part of this international progress, we presented here a considerable variety of contributions, which became feasible thank to gradually generating, multi-year long, critically evaluated, complex and coherent data sets. Dynamic and timing properties of 247 NPF and growth events were studied together with supporting aerosol properties, meteorological data and pollutant gas concentrations in near-city background and city centre of Budapest for 6 years. The results and conclusions derived form in important component that is based on atmospheric observations. The present study can also be considered as the first step toward a larger and more comprehensive statistical evaluation process. ~~The results are to be combine with results from laboratory experiments and finally, with theoretical models to further improve our understanding on the atmospheric processes in cities. Specialities and features of the urban atmospheric NPF and growth phenomena are finally to be also considered when assessing their potentials to increase UF and CCN concentrations or their health implications.~~

~~The present research based on ambient atmospheric measurements provided evidence that some important chemical players in the NPF and growth events are still missing. Considering the results and conclusions of cloud chamber experiments, these factors are expected to be related mainly to oxidation products of VOCs and/or their processes.~~ Further dedicated research including sophisticated measurements, data evaluations and modelling studies is required to

28

871 find and identify ~~additional~~ ~~these~~ chemical species and their processes, and to account their

872 multifactorial role in more detail. Such measurement campaign focusing on chemical

873 composition of molecular clusters, precursors and nucleating vapours by applying recent

874 expedient instruments in Budapest over the months of the highest expected event occurrence

875 has been just realised within a frame of an international cooperation. Its perspective results can

876 hopefully provide additional valuable information for some of the conclusion base on indirect

877 evidence for the time being and can further clarify the overall picture on urban multicomponent

878 nucleation and growth phenomenon.

879

880 *Data availability.* The observational data used in this paper are available on request from the

881 corresponding author or at the website of the Budapest platform for Aerosol Research and Training

882 (http://salma.web.elte.hu/BpART).

883

884 *Author contributions.* I.S. designed the study, performed most of the data analysis, interpreted the

885 results and wrote the paper. Z.N. performed most measurements and data treatment, and contributed to

886 the data analysis.

887

888 *Competing interest.* The authors declare that they have no conflict of interest.

889

894

References

896 Alam, A., Shi, J. P., and Harrison, R. M.: Observations of new particle formation in urban air, J.

897   Geophys. Res., 108 (D3), 4093, doi:10.1029/2001JD001417, 2003.

898 Almeida, J., Schobesberger, S., Kurten, A., Ortega, I. K., Kupiainen-Maatta, O., Praplan, A. P.,

899   Adamov, A., Amorim, A., Bianchi, F., Breitenlechner, M., David, A., Dommen, J., Donahue, N.

900   M., Downard, A., Dunne, E., Duplissy, J., Ehrhart, S., Flagan, R. C., Franchin, A., Guida, R.,

901   Hakala, J., Hansel, A., Heinritzi, M., Henschel, H., Jokinen, T., Junninen, H., Kajos, M.,

902   Kangasluoma, J., Keskinen, H., Kupc, A., Kurten, T., Kvashin, A. N., Laaksonen, A., Lehtipalo,

903   K., Leiminger, M., Leppa, J., Loukonen, V., Makhmutov, V., Mathot, S., McGrath, M. J.,

904   Nieminen, T., Olenius, T., Onnela, A., Petäjä, T., Riccobono, F., Riipinen, I., Rissanen, M., Rondo,

905   L., Ruuskanen, T., Santos, F. D., Sarnela, N., Schallhart, S., Schnitzhofer, R., Seinfeld, J. H.,

906   Simon, M., Sipilä, M., Stozhkov, Y., Stratmann, F., Tome, A., Tröstl, J., Tsagkogeorgas, G.,

907   Vaattovaara, P., Viisanen, Y., Virtanen, A., Vrtala, A., Wagner, P. E., Weingartner, E., Wex, H.,

908   Williamson, C., Wimmer, D., Ye, P. L., Yli-Juuti, T., Carslaw, K. S., Kulmala, M., Curtius, J.,

909   Baltensperger, U., Worsnop, D. R., Vehkamäki, H., and Kirkby, J.: Molecular understanding of

910   sulphuric acid–amine particle nucleation in the atmosphere, Nature, 502, 359–363, 2013.

911   Baltensperger, U., Streit, N., Weingartner, E., Nyeki, S., Prévôt, A. S. H., Van Dingenen, R., Virkkula,

912   A., Putaud, J. P., Even, A., Brink, H., Blatter, A., Neftel, A., and Gaggeler, H. W.: Urban and rural

913   aerosol characterization of summer smog events during the PIPAPO field campaign in Milan, Italy,

914   J. Geophys. Res., 107(D22), 8193, doi:10.1029/2001JD001292, 2002.

915   Bianchi, F., Tröstl, J., Junninen, H., Frege, C., Henne, S., Hoyle, C. R., Molteni, U., Herrmann, E.,

916   Adamov, A., Bukowiecki, N., Chen, X., Duplissy, J., Gysel, M., Hutterli, M. Kangasluoma, J.,

917   Kontkanen, J., Kürten, A. Manninen, H. E., Münch, S., Peräkylä, O., Petäjä, T., Rondo, L.,

918   Williamson, C., Weingartner, E. Curtius, J., Worsnop, D. R., Kulmala, M., Dommen, J., and

919   Baltensperger, U.: New particle formation in the free troposphere: A question of chemistry and

920   timing, Science, 352, 1109–1112, https://doi.org/10.1126/science.aad5456, 2016.

921   Braakhuis, H. M., Park, M. V., Gosens, I., De Jong, W. H., and Cassee, F. R.: Physicochemical

922   characteristics of nanomaterials that affect pulmonary inflammation, Part. Fibre Toxicol., 11:18,

923   doi: 10.1186/1743-8977-11-18, 2014.

924   Cai, R. and Jiang, J.: A new balance formula to estimate new particle formation rate: reevaluating the

925   effect of coagulation scavenging, Atmos. Chem. Phys., 17, 12659–12675, 2017.

926   Carslaw, K. S., Lee, L. A., Reddington, C. L., Pringle, K. J., Rap, A., Forster, P. M., Mann, G. W.,

927   Spracklen, D. V., Woodhouse, M. T., Regayre, L. A., and Pierce, J. R: Large contribution of

928   natural aerosols to uncertainty in indirect forcing, Nature, 503, 67–71, 2013.

929   Crounse, J. D., Nielsen, L. B., Jørgensen, S., Kjaergaard, H. G., and Wennberg, P. O.: Autoxidation of

930   organic compounds in the atmosphere, J. Phys. Chem. Lett., 4, 20, 3513–3520, 2013.

931   Dal Maso, M., Kulmala, M., Lehtinen, K. E. J., Mäkelä, J. M., Aalto, P. P., and O'Dowd, C.:

932   Condensation and coagulation sinks and formation of nucleation mode particles in coastal and

933   boreal forest boundary layers, J. Geophys. Res., 107(19D), 8097, 10.1029/2001jd001053, 2002.

934   Dal Maso, M., Kulmala, M., Riipinen, I., Wagner, R., Hussein, T., Aalto, P. P., and Lehtinen, K. E. J.:

935   Formation and growth of fresh atmospheric aerosols: eight years of aerosol size distribution data

936   from SMEAR II, Hyytiälä, Finland, Boreal Environ. Res., 10, 323–336, 2005.

937   Dall'Osto, M., Querol, X., Alastuey, A., O'Dowd, C., Harrison, R. M., Wenger, J., and Gómez-

938   Moreno, F. J.: On the spatial distribution and evolution of ultrafine particles in Barcelona, Atmos.

939   Chem. Phys., 13, 741–759, 2013.

940   Ehn, M., Thornton, J. A., Kleist, E., Sipilä, M., Junninen, H., Pullinen, I., Springer, M., Rubach, F.,

941   Tillmann, R., Lee, B., Lopez-Hilfiker, F., Andres, S., Acir, I. H., Rissanen, M., Jokinen, T.,

942   Schobesberger, S., Kangasluoma, J., Kontkanen, J., Nieminen, T., Kurten, T., Nielsen, L. B.,

943   Jorgensen, S., Kjaergaard, H. G., Canagaratna, M., Dal Maso, M., Berndt, T., Petäjä, T., Wahner,

944   A., Kerminen, V. M., Kulmala, M., Worsnop, D. R., Wildt, J., and Mentel, T. F.: A large source of

945   low-volatility secondary organic aerosol, Nature, 506, 476–479, 2014.

946 Gordon, H., Sengupta, K., Rap, A., Duplissy, J., Frege, C., Williamson, C., Heinritzi, M., Simon, M.,

947   Yan, C., Almeida, J., Tröstl, J., Nieminen, T., Ortega, I. K., Wagner, R., Dunne, E. M., Adamov,

948   A., Amorim, A., Bernhammer, A. K., Bianchi, F., Breitenlechner, M., Brilke, S., Chen, X., Craven,

949   J. S., Dias, A., Ehrhart, S., Fischer, L., Flagan, R. C., Franchin, A., Fuchs, C., Guida, R., Hakala, J.,

950   Hoyle, C. R., Jokinen, T., Junninen, H., Kangasluoma, J., Kim, J., Kirkby, J., Krapf, M., Kürten,

951   A., Laaksonen, A., Lehtipalo, K., Makhmutov, V., Mathot, S., Molteni, U., Monks, S. A., Onnela,

952   A., Peräkylä, O., Piel, F., Petäjä, T., Praplan, A. P., Pringle, K. J., Richards, N. A. D., Rissanen, M.

953   P., Rondo, L., Sarnela, N., Schobesberger, S., Scott, C. E., Seinfeld, J. H., Sharma, S., Sipilä, M.,

954   Steiner, G., Stozhkov, Y., Stratmann, F., Tomé, A., Virtanen, A., Vogel, A. L., Wagner, A. C.,

955   Wagner, P. E., Weingartner, E., Wimmer, D., Winkler, P. M., Ye, P., Zhang, X., Hansel, A.,

956   Dommen, J., Donahue, N. M., Worsnop, D. R., Baltensperger, U., Kulmala, M., Curtius, J., and

957   Carslaw, K. S.: Reduced anthropogenic aerosol radiative forcing caused by biogenic new particle

958   formation, Proc. Natl. Acad. Sci. U.S.A., 113, 12053–12058,

959   https://doi.org/10.1073/pnas.1602360113, 2016.

960 Hamed, A., Korhonen, H., Sihto, S.-L., Joutsensaari, J., Järvinen, H., Petäjä, T., Arnold, F., Nieminen,

961   T., Kulmala, M., Smith, J. N., Lehtinen, K. E. J., and Laaksonen, A.: The role of relative humidity

962   in continental new particle formation. J. Geophys. Res., 116, D03202, doi:10.1029/2010JD014186,

963   2011.

964 Hirsikko, A., Vakkari, V., Tiitta, P., Hatakka, J., Kerminen, V.-M., Sundström, A.-M., Beukes, J. P.,

965   Manninen, H. E., Kulmala, M., and Laakso, L.: Multiple daytime nucleation events in semi-clean

966   savannah and industrial environments in South Africa: analysis based on observations, Atmos.

967   Chem. Phys., 13, 5523–5532, 2013.

968 Hussein, T., Puustinen, A., Aalto, P. P., Mäkelä, J. M., Hämeri, K., and Kulmala, M.: Urban aerosol

969   number size distributions, Atmos. Chem. Phys., 4, 391–411, 2004.

970 Hussein, T., Martikainen, J., Junninen, H., Sogacheva, L., Wagner, R., Dal Maso, M., Riipinen, I.,

971   Aalto, P. P., and Kulmala, M.: Observation of regional new particle formation in the urban

972   atmosphere, Tellus 60B, 509–521, 2008.

973 Jokinen, T., Berndt, T., Makkonen, R., Kerminen, V.-M., Junninen, H., Paasonen, P., Stratmann, F.,

974   Herrmann, H., Guenther, A. B., Worsnop, D. R., Kulmala, M., Ehn, M. and Sipilä, M.: Production

975   of extremely low volatile organic compounds from biogenic emissions: Measured yields and

976   atmospheric implications, Proc. Natl. Acad. Sci. U.S.A., 112, 7123–7128, 2015.

977 Kerminen, V.-M., Paramonov, M., Anttila, T., Riipinen, I., Fountoukis, C., Korhonen, H., Asmi, E.,

978   Laakso, L., Lihavainen, H., Swietlicki, E., Svenningsson, B., Asmi, A., Pandis, S. N., Kulmala, M.,

979   and Petäjä, T.: Cloud condensation nuclei production associated with atmospheric nucleation: a

980   synthesis based on existing literature and new results, Atmos. Chem. Phys., 12, 12037–12059,
981   2012.

982 Kerminen, V.-M., Chen, X., Vakkari, V., Petäjä, T., Kulmala, M., and Bianchi, F.: Atmospheric new
983   particle formation and growth: review of field observations, Environ. Res. Lett., 13 (2018) 103003,
984   2018.

985 Kiendler-Scharr, A., Wildt, J., Dal Maso, M., Hohaus, T., Kleist, E., Mentel, T. F., Tillmann, R.,
986   Uerlings, R., Schurr, U., and Wahner, A.: New particle formation in forests inhibited by isoprene
987   emissions. Nature, 461, 381–384, 2009.

988 Kirkby, J., Curtius, J., Almeida, J., Dunne, E., Duplissy, J., Ehrhart, S., Franchin, A., Gagné, S., Ickes,
989   L., Kürten, A., Kupc, A., Metzger, A., Riccobono, F., Rondo, L., Schobesberger, S.,
990   Tsagkogeorgas, G., Wimmer, D., Amorim, A., Bianchi, F., Breitenlechner, M., David, A.,
991   Dommen, J., Downard, A., Ehn, M., Flagan, R. C., Haider, S., Hansel, A., Hauser, D., Jud, W.,
992   Junninen, H., Kreissl, F., Kvashin, A., Laaksonen, A., Lehtipalo, K., Lima, J., Lovejoy, E. R.,
993   Makhutov, V., Mathot, S., Mikkilä, J., Minginette, P., Mogo, S., Nieminen, T., Onnela, A., Pereira,
994   A., Petäjä, T., Schnitzhofer, R., Seinfeld, J. H., Sipilä, M., Stozhkov, Y., Stratmann, F., Tome, A.,
995   Vanhanen, J., Viisanen Y., Vrtala, A., Wagner, P.E., Walther, H., Weingartner, E., Wex, H.,
996   Winkler, P.M., Carslaw, K. S., Worsnop, D. R., Baltensperger, U., and Kulmala, M.: The role of
997   sulfuric acid, ammonia and galactic cosmic rays in atmospheric aerosol nucleation, Nature, 476,
998   429–433, 2011.

999 Kirkby, J., Duplissy, J., Sengupta, K., Frege, C., Gordon, H., Williamson, C., Heinritzi, M., Simon,
1000   M., Yan, C., Almeida, J., Tröstl, J., Nieminen, T., Ortega, I. K., Wagner, R., Adamov, A., Amorim,
1001   A., Bernhammer, A.-K., Bianchi, F., Breitenlechner, M., Brilke, S., Chen, X., Craven, J., Dias, A.,
1002   Ehrhart, S., Flagan, R. C., Franchin, A., Fuchs, C., Guida, R., Hakala, J., Hoyle, C. R., Jokinen, T.,
1003   Junninen, H., Kangasluoma, J., Kim, J., Krapf, M., Kürten, A., Laaksonen, A., Lehtipalo, K.,
1004   Makhmutov, V., Mathot, S., Molteni, U., Onnela, A., Peräkylä, O., Piel, F., Petäjä, T., Praplan, A.
1005   P., Pringle, K., Rap, A., Richards, N. A. D., Riipinen, I., Rissanen, M. P., Rondo, L., Sarnela, N.,
1006   Schobesberger, S., Scott, C. E., Seinfeld, J. H., Sipilä, M., Steiner, G., Stozhkov, Y., Stratmann, F.,
1007   Tomé, A., Virtanen, A., Vogel, A. L., Wagner, A., Wagner, P. E., Weingartner, E., Wimmer, D.,
1008   Winkler, P. M., Ye, P., Zhang, X., Hansel, A., Dommen, J., Donahue, N. M., Worsnop, D. R.,
1009   Baltensperger, U., Kulmala, M., Carslaw, K. S., and Curtius, J.: Ion-induced nucleation of pure
1010   biogenic particles, Nature, 533, 521–526, https://doi.org/10.1038/nature17953, 2016.

1011 Kulmala, M., Dal Maso, M., Mäkelä, J. M., Pirjola, L., Väkevä, M., Aalto, P., Miikkulainen, P.,
1012   Hämeri, K., and O'Dowd, C. D.: On the formation, growth and composition of nucleation mode
1013   particles, Tellus B53, 479–490, 2001.

1014 Kulmala, M., Vehkamäki, H., Petäjä, T., Dal Maso, M., Lauri, A., Kerminen, V.-M., Birmili, W., and
1015   McMurry, P.: Formation and growth rates of ultrafine atmospheric particles: a review of
1016   observations, J. Aerosol Sci., 35, 143–176, 2004.

1017   Kulmala, M., Petäjä, T., Nieminen, T., Sipilä, M., Manninen, H. E., Lehtipalo, K., Dal Maso, M.,

1018   Aalto, P. P., Junninen, H., Paasonen, P., Riipinen, I., Lehtinen, K. E. J., Laaksonen, A., and

1019   Kerminen, V.-M.: Measurement of the nucleation of atmospheric aerosol particles, Nat. Protoc., 7,

1020   1651–1667, doi:10.1038/nprot.2012.091, 2012.

1021   Kulmala, M., Kontkanen, J., Junninen, H., Lehtipalo, K., Manninen, H. E., Nieminen, T., Petäjä, T.,

1022   Sipilä, M., Schobesberger, S., Rantala, P., Franchin, A., Jokinen, T., Järvinen, E., Äijälä, M.,

1023   Kangasluoma, J., Hakala, J., Aalto, P.P., Paasonen, P., Mikkilä, J., Vanhanen, J., Aalto, J., Hakola,

1024   H., Makkonen, U., Ruuskanen, T., Mauldin, R. L. III, Duplissy, J., Vehkamäki, H., Bäck, J.,

1025   Kortelainen, A., Riipinen, I., Kurtén, T., Johnston, M. V., Smith, J. N., Ehn, M., Mentel, T. F.,

1026   Lehtinen, K. E. J., Laaksonen, A., Kerminen, V.-M., and Worsnop, D. R.: Direct observations of

1027   atmospheric aerosol nucleation, Science, 339, 943–946, 2013.

1028   Kulmala, M., Petäjä, T., Ehn, M., Thornton, J., Sipilä, M., Worsnop, D. R., and Kerminen, V.-M.:

1029   Chemistry of atmospheric nucleation: On the recent advances on precursor characterization and

1030   atmospheric cluster composition in connection with atmospheric new particle formation, Annu.

1031   Rev. Phys. Chem., 65, 21−37, 2014.

1032   Kulmala, M., Kerminen, V. M., Petäjä, T., Ding, A. J., and Wang, L.: Atmospheric gas-to-particle

1033   conversion: why NPF events are observed in megacities, Faraday Discuss.,

1034   doi:10.1039/C6FD00257A, 2017.

1035   Makkonen, R., Asmi, A., Korhonen, H., Kokkola, H., Järvenoja, S., Räisänen, P., Lehtinen, K. E. J.,

1036   Laaksonen, A., Kerminen, V.-M., Järvinen, H., Lohmann, U., Bennartz, R., Feichter, J., and

1037   Kulmala, M.: Sensitivity of aerosol concentrations and cloud properties to nucleation and

1038   secondary organic distribution in ECHAM5-HAM global circulation model, Atmos. Chem. Phys.,

1039   9, 1747–1766, 2009.

1040   Makkonen, R., Asmi, A., Kerminen, V.-M., Boy, M., Arneth, A., Hari, P., and Kulmala, M.: Air

1041   pollution control and decreasing new particle formation lead to strong climate warming, Atmos.

1042   Chem. Phys., 12, 1515–1524, 2012.

1043   Merikanto, J., Spracklen, D. V., Mann, G. W., Pickering, S. J., and Carslaw, K. S.: Impact of

1044   nucleation on global CCN, Atmos. Chem. Phys., 9, 8601–8616, 2009.

1045   Metzger, A., Verheggen, B., Dommen, J., Duplissy, J., Prévôt, A. S. H., Weingartner, E., Riipinen, I.,

1046   Kulmala, M., Spracklen, D. V., Carslaw, K. S., and Baltensperger, U.: Evidence for the role of

1047   organics in aerosol particle formation under atmospheric conditions, Proc. Natl. Acad. Sci. U. S.

1048   A., 107, 6646–6651, 2010.

1049   Németh, Z. and Salma, I.: Spatial extension of nucleating air masses in the Carpathian Basin, Atmos.

1050   Chem. Phys., 14, 8841–8848, 2014.

1051   Németh, Z., Rosati, B., Zíková, N., Salma, I., Bozó, L., Dameto de España, C., Schwarz, J., Ždímal,

1052   V., and Wonaschütz, A.: Comparison of atmospheric new particle formation and growth events in

1053   three Central European cities, Atmos. Environ., 178, 191–197, 2018.

1054 Nieminen, T., Kerminen, V.-M., Petäjä, T., Aalto, P. P., Arshinov, M., Asmi, E., Baltensperger, U.,
1055 Beddows, D. C. S., Beukes, J. P., Collins, D., Ding, A., Harrison, R. M., Henzing, B., Hooda, R.,
1056 Hu, M., Hõrrak, U., Kivekäs, N., Komsaare, K., Krejčí, R., Kristensson, A., Laakso, L., Laaksonen,
1057 A., Leaitch, W. R., Lihavainen, H., Mihalopoulos, N., Németh, Z., Nie, W., O'Dowd, C., Salma, I.,
1058 Sellegri, K., Svenningsson, B., Swietlicki, E., Tunved, P., Ulevicius, V., Vakkari, V., Vana, M.,
1059 Wiedensohler, A., Wu, Z., Virtanen, A., and Kulmala, M.: Global analysis of continental boundary
1060 layer new particle formation based on long-term measurements, Atmos. Chem. Phys., 18, 14737–
1061 14756, 2018.
1062 Oberdörster, G., Oberdörster, E., and Oberdörster, J.: Nanotoxicology: an emerging discipline
1063 evolving from studies of ultrafine particles, Environ. Health Perspect., 113, 823–839, 2005.
1064 O'Dowd, C. D., Jimenez, J. L., Bahreini, R. Flagan, R. C., Seinfeld, J. H., Hämeri, K., Pirjola, L.,
1065 Kulmala, M., Jennings, S. G., and Hoffmann, Th.: Marine aerosol formation from biogenic iodine
1066 emissions, Nature 417, 632–636, 2002.
1067 Paasonen, P., Kupiainen, K., Klimont, Z., Visschedijk, A., Denier van der Gon, H. A. C., and Amann,
1068 M.: Continental anthropogenic primary particle number emissions, Atmos. Chem. Phys., 16, 6823–
1069 6840, 2016.
1070 Paasonen, P., Peltola, M., Kontkanen, J., Junninen, H., Kerminen, V.-M., and Kulmala, M.:
1071 Comprehensive analysis of particle growth rates from nucleation mode to cloud condensation
1072 nuclei in Boreal forest, Atmos. Chem. Phys. Discuss., https://doi.org/10.5194/acp-2018-169, in
1073 review, 2018.
1074 Petäjä, T., Mauldin, III, R. L., Kosciuch, E., McGrath, J., Nieminen, T., Paasonen, P., Boy, M.,
1075 Adamov, A., Kotiaho, T., and Kulmala, M.: Sulfuric acid and OH concentrations in a boreal forest
1076 site, Atmos. Chem. Phys., 9, 7435–7448, 2009.
1077 Putaud, J.-P., Van Dingenen, R., Alastuey, A., Bauer, H., Birmili, W., Cyrys, J., Flentje, H., Fuzzi, S.,
1078 Gehrig, R., Hansson, H. C., Harrison, R. M., Herrmann, H., Hitzenberger, R., Hüglin, C., Jones,
1079 A.M., Kasper-Giebl, A., Kiss, G., Kousa, A., Kuhlbusch, T. A. J., Löschau, G., Maenhaut, W.,
1080 Molnár, A., Moreno, T., Pekkanen, J., Perrino, C., Pitz, M., Puxbaum, H., Querol, X., Rodriguez,
1081 S., Salma, I., Schwarz, J., Smolík, J., Schneider, J., Spindler, G., ten Brink, H., Turšič, J., Viana,
1082 M., Wiedensohler, and A., Raes, F.: A European Aerosol Phenomenology - 3: physical and
1083 chemical characteristics of particulate matter from 60 rural, urban, and kerbside sites across
1084 Europe, Atmos. Environ., 44, 1308–1320, 2010.
1085 Riccobono, F., Schobesberger, S., Scott, C., Dommen, J., Ortega, I., Rondo, L., Almeida, J., Amorim,
1086 A., Bianchi, F., Breitenlechner, M., David, A., Downard, A., Dunne, E., Duplissy, J., Ehrhart, S.,
1087 Flagan, R., Franchin, A., Hansel, A., Junninen, H., Kajos, M., Keskinen, H., Kupc, A., Kurten, A.,
1088 Kvashin, A., Laaksonen, A., Lehtipalo, K., Makhmutov, V., Mathot, S., Nieminen, T., Onnela, A.,
1089 Petäjä, T., Praplan, A., Santos, F., Schallhart, S., Seinfeld, J., Sipila, M., Spracklen, D., Stozhkov,
1090 Y., Stratmann, F., Tome, A., Tsagkogeorgas, G., Vaattovaara, P., Viisanen, Y., Vrtala, A., Wagner,

1091   P., Weingartner, E., Wex, H., Wimmer, D., Carslaw, K., Curtius, J., Donahue, N., Kirkby, J.,

1092   Kulmala, M., Worsnop, D., and Baltensperger, U.: Oxidation products of biogenic emissions

1093   contribute to nucleation of atmospheric particles, Science, 344, 717–721, 2014.

1094   Riipinen, I., Pierce, J. R., Yli-Juuti, T., Nieminen, T., Häkkinen, S., Ehn, M., Junninen, H., Lehtipalo,

1095   K., Petäjä, T., Slowik, J., Chang, R., Shantz, N. C., Abbatt, J., Leaitch, W. R., Kerminen, V.-M.,

1096   Worsnop, D. R., Pandis, S. N., Donahue, N. M., and Kulmala, M.: Organic condensation: a vital

1097   link connecting aerosol formation to cloud condensation nuclei (CCN) concentrations, Atmos.

1098   Chem. Phys., 11, 3865–3878, 2011.

1099   Salma, I., Borsós, T., Weidinger, T., Aalto, P., Hussein, T., Dal Maso, M., and Kulmala, M.:

1100   Production, growth and properties of ultrafine atmospheric aerosol particles in an urban

1101   environment, Atmos. Chem. Phys., 11, 1339–1353, 2011.

1102   Salma, I., Borsós, T., Németh, Z., Weidinger, T., Aalto, T., and Kulmala, M.: Comparative study of

1103   ultrafine atmospheric aerosol within a city, Atmos. Environ., 92, 154–161, 2014.

1104   Salma, I., Füri, P., Németh, Z., Farkas, Á., Balásházy, I., Hofmann, W., and Farkas, Á.: Lung burden

1105   and deposition distribution of inhaled atmospheric urban ultrafine particles as the first step in their

1106   health risk assessment, Atmos. Environ., 104, 39–49, 2015.

1107   Salma, I., Németh, Z., Weidinger, T., Kovács, B., and Kristóf, G.: Measurement, growth types and

1108   shrinkage of newly formed aerosol particles at an urban research platform, Atmos. Chem. Phys.,

1109   16, 7837–7851, 2016a.

1110   Salma, I., Németh, Z., Kerminen, V. M., Aalto, P., Nieminen, T., Weidinger, T., Molnár, Á., Imre, K.,

1111   and Kulmala, M.: Regional effect on urban atmospheric nucleation, Atmos. Chem. Phys., 16,

1112   8715–8728, 2016b.

1113   Salma, I., Varga, V., and Németh, Z.: Quantification of an atmospheric nucleation and growth process

1114   as a single source of aerosol particles in a city, Atmos. Chem. Phys., 17, 15007–15017, 2017.

1115   Schobesberger, S., Junninen, H., Bianchi, F., Lonn, G., Ehn, M., Lehtipalo, K., Dommen, J., Ehrhart,

1116   S., Ortega, I. K., Franchin, A., Nieminen, T., Riccobono, F., Hutterli, M., Duplissy, J., Almeida, J.,

1117   Amorim, A., Breitenlechner, M., Downard, A. J., Dunne, E. M., Flagan, R. C., Kajos, M.,

1118   Keskinen, H., Kirkby, J., Kupc, A., Kurten, A., Kurten, T., Laaksonen, A., Mathot, S., Onnela, A.,

1119   Praplan, A. P., Rondo, L., Santos, F. D., Schallhart, S., Schnitzhofer, R., Sipilä, M., Tome, A.,

1120   Tsagkogeorgas, G., Vehkamäki, H., Wimmer, D., Baltensperger, U., Carslaw, K. S., Curtius, J.,

1121   Hansel, A., Petäjä, T., Kulmala, M., Donahue, N. M., and Worsnop, D. R.: Molecular

1122   understanding of atmospheric particle formation from sulfuric acid and large oxidized organic

1123   molecules, Proc. Natl. Acad. Sci. U.S.A., 110, 17223–17228, 10.1073/pnas.1306973110, 2013.

1124   Sihto, S.-L., Mikkilä, J., Vanhanen, J., Ehn, M., Liao, L., Lehtipalo, K., Aalto, P. P., Duplissy, J.,

1125   Petäjä, T., Kerminen, V.-M., Boy, M., and Kulmala, M.: Seasonal variation of CCN concentrations

1126   and aerosol activation properties in boreal forest, Atmos. Chem. Phys., 11, 13269–13285, 2011.

1127 Sipilä, M., Berndt, T., Petäjä, T., Brus, D., Vanhanen, J., Stratmann, F., Patokoski, J., Mauldin, R. L.
1128   3rd, Hyvärinen, A. P., Lihavainen, H., and Kulmala, M.: The role of sulfuric acid in atmospheric
1129   nucleation, Science, 327(5970), 1243-6. doi: 10.1126/science.1180315, 2010.
1130 Spracklen, D. V., Carslaw, K. S., Merikanto, J., Mann, G. W., Reddington, C. L., Pickering, S., Ogren,
1131   J. A., Andrews, E., Baltensperger, U., Weingartner, E., Boy, M., Kulmala. M., Laakso, L.,
1132   Lihavainen, H., Kivekäs, N., Komppula, M., Mihalopoulos, N., Kouvarakis, G., Jennings, S. G.,
1133   O'Dowd, C., Birmili, W., Wiedensohler, A., Weller, R., Gras, J., Laj, P., Sellegri, K., Bonn, B.,
1134   Krejčí, R., Laaksonen, A., Hamed, A., Minikin, A., Harrison, R. M., Talbot, R., and Sun, J.: The
1135   contribution of boundary layer nucleation events to total particle concentrations on regional and
1136   global scales, Atmos. Chem. Phys., 6, 5631–5648, 2006.
1137 Sun, J., Birmili, W., Hermann, M., Tuch, T., Weinhold, K., Spindler, G.,Schladitz, A., Bastian, S.,
1138   Löschau, G., Cyrys, J., Gu, J., Flentje, H., Briel, B., Asbach, C., Kaminski, H., Ries, L., Sohmer,
1139   R., Gerwig, H., Wirtz, K., Meinhardt, F., Schwerin, A., Bath, O., Ma, N., and Wiedensohler, A.:
1140   Variability of Black Carbon mass concentrations, sub-micrometer particle number concentrations
1141   and size distributions: Results of the German Ultrafine Aerosol Network ranging from city street to
1142   high Alpine locations, Atmos. Environ., 202, 256–268, 2019.
1143 Tröstl, J., Chuang, W. K., Gordon, H., Heinritzi, M., Yan, C., Molteni, U., Ahlm, L., Frege, C.,
1144   Bianchi, F., Wagner, R., Simon, M., Lehtipalo, K., Williamson, C., Craven, J. S., Duplissy, J.,
1145   Adamov, A., Almeida, J., Bernhammer, A. K., Breitenlechner, M., Brilke, S., Dias, A., Ehrhart, S.,
1146   Flagan, R. C., Franchin, A., Fuchs, C., Guida, R., Gysel, M., Hansel, A., Hoyle, C. R., Jokinen, T.,
1147   Junninen, H., Kangasluoma, J., Keskinen, H., Kim, J., Krapf, M., Kürten, A., Laaksonen, A.,
1148   Lawler, M., Leiminger, M., Mathot, S., Möhler, O., Nieminen, T., Onnela, A., Petäjä, T., Piel, F.
1149   M., Miettinen, P., Rissanen, M. P., Rondo, L., Sarnela, N., Schobesberger, S., Sengupta, K., Sipilä,
1150   M., Smith, J. N., Steiner, G., Tomè, A., Virtanen, A., Wagner, A. C., Weingartner, E., Wimmer, D.,
1151   Winkler, P. M., Ye, P. L., Carslaw, K. S., Curtius, J., Dommen, J., Kirkby, J., Kulmala, M.,
1152   Riipinen, I., Worsnop, D. R., Donahue, N. M., and Baltensperger, U.: The role of low-volatility
1153   organic compounds in initial particle growth in the atmosphere, Nature, 533, 527,
1154   10.1038/nature18271, 2016.
1155 Vakkari, V., Tiitta, P., Jaars, K., Croteau, P., Beukes, J. P., Josipovic, M., Kerminen, V.-M., Kulmala,
1156   M., Venter, A. D., van Zyl, P. G., Worsnop, D. R., and Laakso, L.: Reevaluating the contribution of
1157   sulfuric acid and the origin of organic compounds in atmospheric nanoparticle growth, Geophys.
1158   Res. Lett., 42, 10486−10493, 2015.
1159 Vuollekoski, H., Sihto, S.-L., Kerminen, V.-M., Kulmala, M., and Lehtinen, K. E. J.: A numerical
1160   comparison of different methods for determining the particle formation rate, Atmos. Chem. Phys.,
1161   12, 2289–2295, 2012.

1162 Wehner, B., Wiedensohler, A., Tuch, T. M., Wu, Z. J., Hu, M., Slanina, J., and Kiang, C. S.:
1163   Variability of the aerosol number size distribution in Beijing, China: new particle formation, dust
1164   storms, and high continental background, Geophys. Res. Lett., 31, L22108, 2004.
1165 Wiedensohler, A., Cheng, Y. F., Nowak, A., Wehner, B., Achtert, P., Berghof, M., Birmili, W., Wu, Z.
1166   J., Hu, M., Zhu, T., Takegawa, N., Kita, K., Kondo, Y., Lou, S. R., Hofzumahaus, A., Holland, F.,
1167   Wahner, A., Gunthe, S. S., Rose, D., Su, H., and Pöschl, U.: Mobility particle size spectrometers:
1168   harmonization of technical standards and data structure to facilitate high quality long-term
1169   observations of atmospheric particle number size distributions, Atmos. Meas. Tech., 5, 657–685,
1170   2012.
1171 Woo, K. S., Chen, D. R., Pui, D. Y. H., and McMurry, P. H.: Measurement of Atlanta aerosol size
1172   distributions: observations of ultrafine particle events, Aerosol Sci. Technol., 34, 75–87, 2001.
1173 Xiao, S., Wang, M. Y., Yao, L., Kulmala, M., Zhou, B., Yang, X., Chen, J. M., Wang, D. F., Fu, Q.
1174   Y., Worsnop, D. R., and Wang, L.: Strong atmospheric new particle formation in winter in urban
1175   Shanghai, China, Atmos. Chem. Phys., 15, 1769–1781, 2015.
1176 Yli-Juuti, T., Riipinen, I., Aalto, P. P., Nieminen, T., Maenhaut, W., Janssens, I. A., Claeys, M.,
1177   Salma, I., Ocskay, R., Hoffer, A., Imre, K., and Kulmala, M.: Characteristics of new particle
1178   formation events and cluster ions at K-puszta, Hungary. Boreal Environ. Res., 14, 683–698, 2009.
1179 Zhang, R., Wang, G., Guo, S., Zamora, M. L., Ying, Q., Lin, Y., Wang, W., Hu, M., and Wang, Y.:
1180   Formation of urban fine particulate matter, Chem. Rev., 115, 3803−3855, 2015.

1181 **Supplementary material**

1182

1183 **Table S1.** Relative contributions of particle number concentration increment ($dN_{nuc}/dt=dN_{6-25}/dt-$
1184 $dN_{Ai,<25}/dt$), coagulation scavenging loss (F_{coag}) and growth out of particles from the diameter interval
1185 of 6–25 nm (F_{growth}) relative to the formation rate J_6 in the near-city background and city centre
1186 separately for 1-year long measurement time intervals. The measurement year and number of
1187 quantifiable ~~(class 1A) new aerosol particle formation~~NPF and growth events (n) are also shown.

1188

Environment and year/ statistics	Contribution in %		
	dN_{nuc}/dt	F_{coag}	F_{growth}
Background, 2012–2013, n=43			
Minimum	45	4	2
Maximum	93	38	26
Mean	76	14	10
St. deviation	12	9	5
Centre, 2008–2009, n=31			
Minimum	32	13	3
Maximum	84	44	38
Mean	54	29	18
St. deviation	13	8	9
Centre, 2013–2014, n=48			
Minimum	43	9	3
Maximum	86	37	30
Mean	63	22	15
St. deviation	11	7	7
Centre, 2014–2015, n=56			
Minimum	45	6	2
Maximum	91	46	32
Mean	70	17	14
St. deviation	12	7	8
Centre, 2015–2016, n=17			
Minimum	50	4	2
Maximum	92	43	30
Mean	74	14	11
St. deviation	11	9	8
Centre, 2017–2018, n=52			
Minimum	44	4	3
Maximum	93	41	31
Mean	70	17	13
St. deviation	11	8	7

1189

Table S2. Ranges, averages and standard deviations of condensation sink value during the nucleation
process, daily maximum gas-phase H_2SO_4 proxy, daily mean air temperature and daily mean relative
humidity on quantifiable ~~(class 1A) new particle formation~~NPF and growth events in the near-city
background and city centre separately for the 1-year long measurement time intervals and for the joint
5-year long city centre data set.

| Environment	Background	Centre					
Time interval	2012–2013	2008–2009	2013–2014	2014–2015	2015–2016	2017–2018	All 5 years
Condensation sink, CS (10^{-3} s^{-1})							
Minimum	1.63	3.1	2.0	2.4	1.69	2.1	1.69
Median	5.6	9.5	9.9	8.6	5.0	8.4	8.9
Maximum	14.6	21	17.8	21	18.4	18.5	21
Mean	6.2	11.0	10.4	9.4	6.8	8.7	9.4
St. deviation	3.1	4.9	3.7	4.2	4.2	4.6	4.3
Gas-phase H_2SO_4 proxy (10^4 µg m^{-5} W s)							
Minimum	40	10.9	12.2	5.8	34	7.3	5.8
Median	93	39	40	38	79	46	41
Maximum	163	96	139	135	190	134	190
Mean	93	39	45	42	82	50	48
St. deviation	32	17	27	23	38	31	29
Air temperature, T (°C)							
Minimum	−5.2	−0.46	−1.78	−1.19	−1.07	1.21	−1.78
Median	11.5	17.1	16.8	15.3	14.2	16.7	16.1
Maximum	27	23	28	28	28	27	28
Mean	11.5	16.3	15.7	15.0	13.6	16.4	15.5
St. deviation	8.1	5.6	6.9	7.2	8.3	6.5	6.8
Relative humidity, RH (%)							
Minimum	41	32	41	31	39	36	31
Median	63	49	60	50	55	52	53
Maximum	91	74	78	77	89	73	89
Mean	64	51	60	50	56	52	54
St. deviation	12	11	10	9	12	9	11

1196

1197 **Table S3.** Ranges, averages and standard deviations of daily median concentrations of SO_2, O_3, NO_x
1198 and CO gases on quantifiable ~~(class 1A) new particle formation~~NPF and growth event days in the near-
1199 city background and city centre separately for the 1-year long measurement time intervals and for the
1200 joint 5-year long city centre data set.
1201

Environment	Background	Centre					
Time interval	2012–2013	2008–2009	2013–2014	2014–2015	2015–2016	2017–2018	All 5 years
SO_2 concentration ($\mu g\ m^{-3}$)							
Minimum	4.4	3.4	2.0	0.90	3.3	0.80	0.80
Median	6.2	5.3	5.1	3.9	5.2	3.7	4.8
Maximum	11.7	8.3	8.2	10.4	11.4	7.0	11.4
Mean	6.5	5.4	5.1	4.4	5.9	3.9	4.7
St. deviation	1.4	1.2	1.8	2.4	2.4	1.8	2.1
O_3 concentration ($\mu g\ m^{-3}$)							
Minimum	8.7	1.80	0.80	10.3	13.0	3.7	0.80
Median	61	44	25	35	36	29	31
Maximum	85	93	67	66	61	68	93
Mean	55	39	28	33	37	31	33
St. deviation	21	28	19	14	14	17	19
NO_x concentration ($\mu g\ m^{-3}$)							
Minimum	4.9	13.0	34	32	30	17.8	13.0
Median	12.2	49	72	87	72	75	74
Maximum	66	213	143	186	120	167	213
Mean	15.8	62	77	96	76	79	81
St. deviation	12.1	42	28	41	24	33	38
CO concentration ($mg\ m^{-3}$)							
Minimum	0.167	0.26	0.30	0.26	0.29	0.20	0.198
Median	0.31	0.48	0.56	0.54	0.42	0.52	0.51
Maximum	0.87	0.76	0.79	0.95	0.88	0.86	0.95
Mean	0.38	0.47	0.54	0.55	0.46	0.51	0.52
St. deviation	0.18	0.13	0.14	0.16	0.16	0.15	0.15

1202
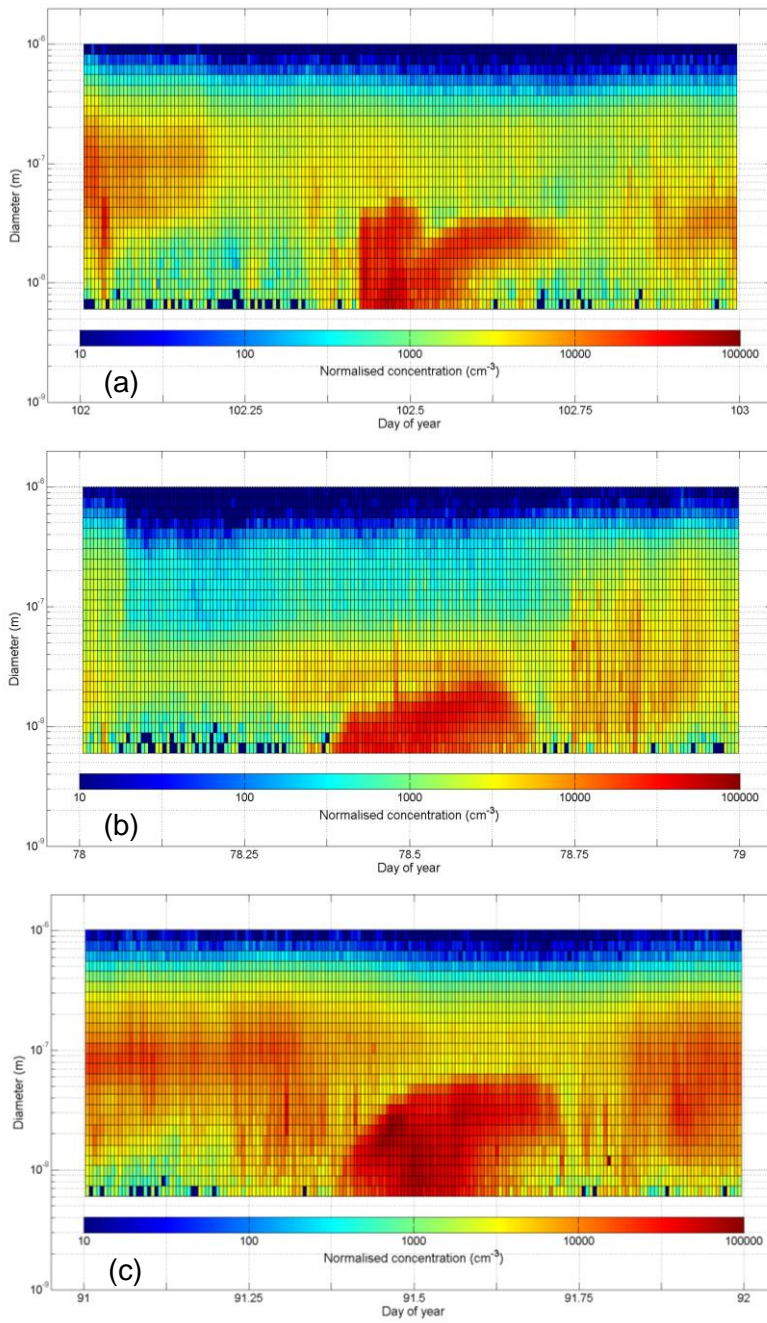
Figure S1. Size distribution surface plots for ~~new aerosol particle formation~~NPF and consecutive particle diameter growth process as banana-shape plots with an emission interference on 12–04–2015 (a), with limited growth of particles on 19–03–2017 (b) and with a broad unresolvable onset on 01–04– 2017 (c) in the city centre.
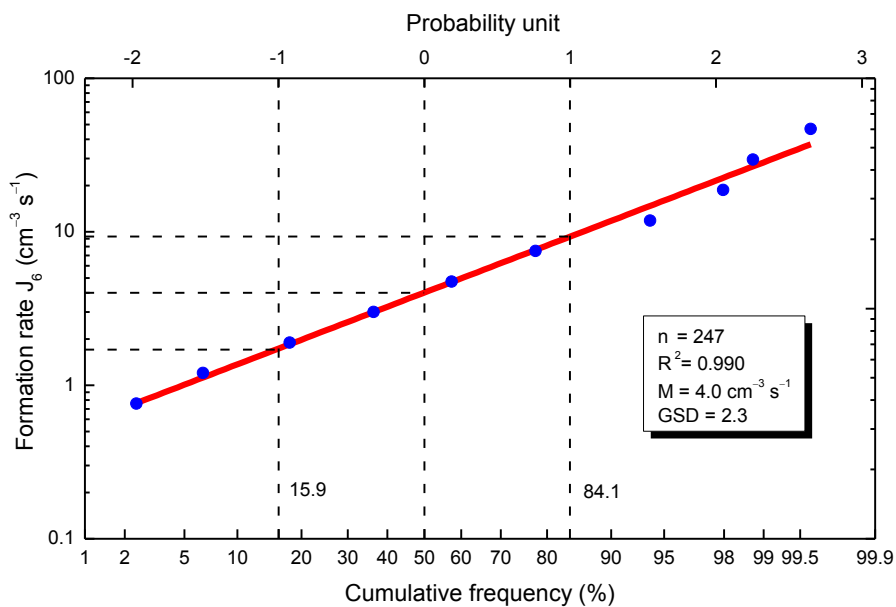
Figure S2. Log-probability graph of the formation rate J_6 and its cumulative frequency distribution for n individual data in the joint overall data set. The linear line in red represents the apparent fit to the data. Coefficient of determination (R^2), median J_6 value (M) and its geometric standard deviation (GSD) obtained from the fitted line are also shown.